SIMULATION, GUIDANCE AND NAVIGATION OF THE B-737 FOR ROLLOUT AND TURNOFF USING MLS MEASUREMENTS

S. Pines
S. F. Schmidt
F. Mann

prepared for

NASA/Langley Research Center
Hampton, Virginia 23665

AMA Report No. 75-40
Contract NAS1-13746
December 8, 1975

ANALYTICAL MECHANICS ASSOCIATES, INC.

50 Jericho Turnpike
Jericho, N. Y. 11753

SUMMARY

This report contains a description for a simulation program for the B-737 aircraft in landing approach, touchdown, rollout and turnoff for normal and CAT III weather conditions. Preliminary results indicate that MLS can be used in place of ILS landing aids and that a single magnetic cable can be used for automated rollout and turnoff. Recommendations are made for further refinement of the model and additional testing to finalize a set of guidance laws for rollout and turnoff.

TABLE OF CONTENTS

LIST OF TABLES

LIST OF FIGURES

LIST OF FIGURES (continued)

NOTATION

ϕ, θ, ψ	=	Euler angles for roll, pitch and yaw
σ	=	Relative yaw between aircraft and runway
$\hat{a}_1, \hat{a}_2, \hat{a}_3$	=	Aircraft unit body axis vectors on the runway system
$R, \dot{R}, \ddot{R}$	=	Aircraft position, velocity and acceleration vectors in the runway system
V	=	Aircraft velocity relative to the atmosphere
W, G, S	=	Wind, gust and shear vectors
G	=	Gravity acceleration
C_D, C_L, C_Y	=	Effective drag, lift and side force coefficients
k	=	Thrust magnitude
m	=	Aircraft mass
ρ	=	Air density
$s, \bar{c}, \bar{b}$	=	Aircraft reference wing area, mean aerodynamic chord and wing span
α_o	=	Angle offset of the thrust direction
F_x, F_y, F_z	=	Landing gear forces
α, β	=	Aerodynamic angle of attack for lift and side force
C_i	=	Aerodynamic coefficients for forces and moments
δ_{spb}	=	Speed brake deflection
δ_R	=	Rudder deflection
δ_{sp}	=	Spoiler deflection
δ_{ST}	=	Stabilizer deflection

δ_e = Elevator deflection

δ_a = Aileron deflection

p, q, r = Aircraft roll rate, pitch rate and yaw rate

I_{ij} = Aircraft inertial moments of mass

M_x, M_y, M_z = Landing gear moments

C.G. = Center of mass in percent of MAC (25% = .25)

μ = Tire coefficient of friction

f_x, f_y, f_z = Specific force measurements from body accelerometers.

ΔT = IMU readout interval; also integration interval

C_M, C_ℓ, C_N = Pitch, roll and yaw aerodynamic coefficients

$C_{D_{G.E.}}, C_{L_{G.E.}}$ = Ground effects aerodynamics coefficients

$C_{D_{GEAR}}, C_{L_{GEAR}}$ = Landing gear aerodynamic coefficients

q_g = Effective pitch rate due to gust

r_g = Effective yaw rate due to gust

p_g = Effective roll rate due to gust

$\hat{a}_i XV$ = Vector cross product of $\hat{a}_i$ and V

F_{pi} = Tire Pressure

p_{ri} = Rated tire pressure

p_i = Tire pressure

w_i = Tire width

d_i = Wheel diameter

I. AIRCRAFT DYNAMICS

This section contains the derivation of the equations used in this study to model the aircraft motion during the landing approach covering the phases of capture, decrab and flare as well as the landing gear and tire dynamics for touchdown, rollout and turnoff.

(a) Choice of the Coordinate Systems. It is customary to utilize linearized equations of motion (Ref. [1]) describing the deviation of the aircraft from a constant speed, fixed flight path angle, wings level equilibrium condition, in the body-stability axes system. While this is sufficient for the landing approach phase, it is inadequate for the rollout and turnoff due to the large deviation in air speed, flight path angle and the large changes in yaw during turnoff. In order to accommodate the broad spectrum of conditions it was decided to use the full non-linear equations of motion in a runway cartesian coordinate system to describe the linear acceleration of the aircraft and to use the body axis and the Euler angle of roll, pitch and yaw to describe the angular acceleration equations.

Since the full non-linear variation of the aerodynamic coefficients is small over the range of Mach numbers and aircraft altitudes in landing, and since the aerodynamic forces during rollout and turnoff become relatively unimportant when compared to the landing gear and thrust forces and moments, it was decided to use a simplified form of constant lift, drag and moment coefficients, fitted to the B-737 for the landing simulation. Numerical values of these aerodynamic coefficients were obtained from Langley Research Center and are given in Table 1. (See pgs. 10-11)

The orientation and sign convention for the runway inertial cartesian coordinate system is given in Figure 1. The aircraft position vector, $R(x, y, z)$, is measured relative to the origin fixed on the center line of the runway with the positive x axis pointing forward along the runway center line. The z axis is positive down, and the y axis is positive to the right in a right-handed orthogonal coordinate system.

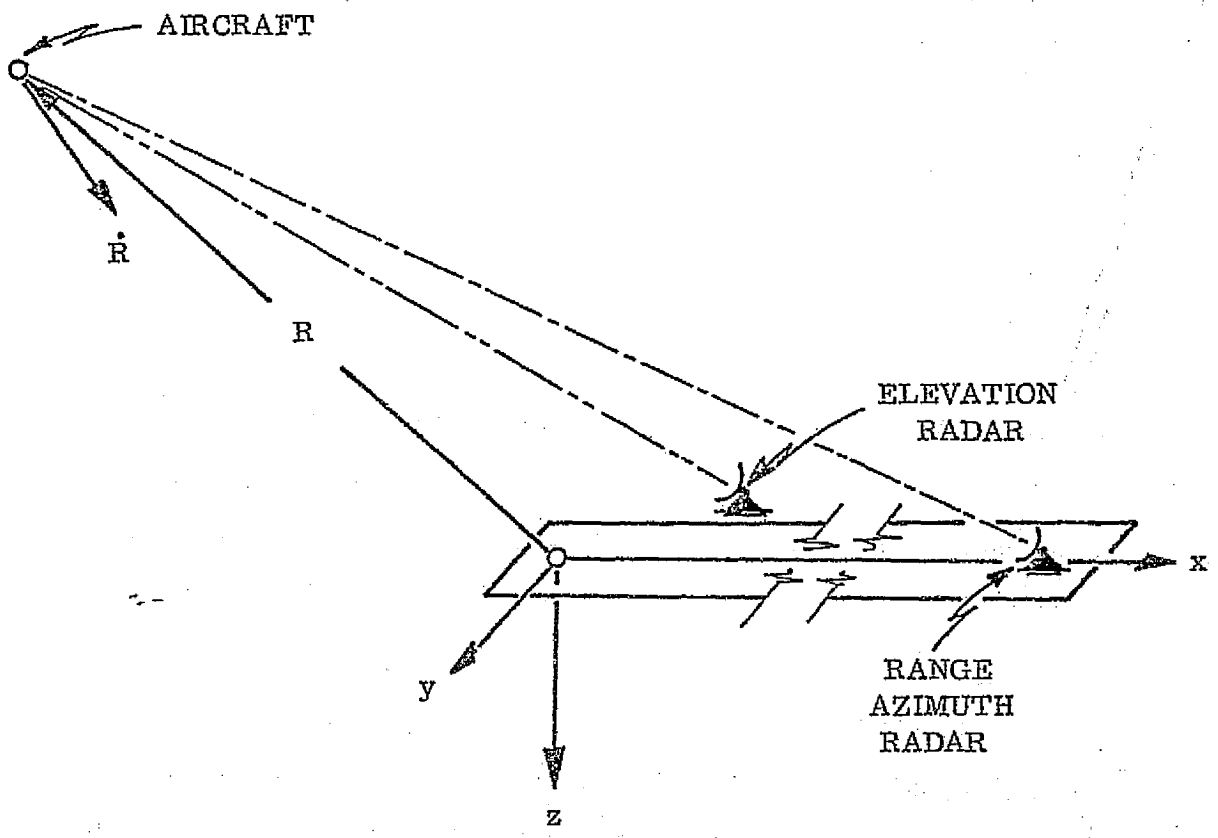

Figure 1. Runway (Inertial) Coordinates and Aircraft Position, Velocity Vectors (R, $\dot{R}$).

The unit vectors $\hat{a}_1$, $\hat{a}_2$, and $\hat{a}_3$ are the unit body axis vectors, lying along the x, y, and z body axes, respectively, expressed in the runway coordinate system in terms of the Euler angles (φ, θ, σ). See Figs. 2a and 2b. The $\hat{a}_1$ axis is along the aircraft center line, positive, forward.

$$\hat{a}_1 = \begin{Bmatrix} \cos\theta\cos\sigma \\ \cos\theta\sin\sigma \\ -\sin\theta \end{Bmatrix} \tag{1}$$

where σ is the difference in yaw between the aircraft and runway,

$$\sigma = \psi - \psi_R \tag{1a}$$

The $\hat{a}_2$ axis is the lateral aircraft axis positive, pointing along the right wing.

$$\hat{a}_2 = \begin{Bmatrix} -\sin\sigma\cos\varphi + \cos\sigma\sin\varphi\sin\theta \\ \cos\sigma\cos\varphi + \sin\sigma\sin\varphi\sin\theta \\ \sin\varphi\cos\theta \end{Bmatrix} \tag{1b}$$

The $\hat{a}_3$ axis is vertical body axis pointing positive downward.

$$\hat{a}_3 = \begin{Bmatrix} \sin\sigma\sin\varphi + \cos\sigma\cos\varphi\sin\theta \\ -\cos\sigma\sin\varphi + \sin\sigma\cos\varphi\sin\theta \\ \cos\varphi\cos\theta \end{Bmatrix} \tag{1c}$$

(b) The Aircraft Equation of Motion. The aircraft inertial velocity vector, $\dot{R}(\dot{x}, \dot{y}, \dot{z})$ is given by the time rate of change of the position vector

$$\frac{d}{dt} R = \dot{R} \tag{2}$$

The vector velocity of the aircraft relative to the atmosphere $V(v_1, v_2, v_3)$ is given by the aircraft inertial velocity vector and the winds.

$$V = \dot{R} - W + G + S \tag{3}$$

where

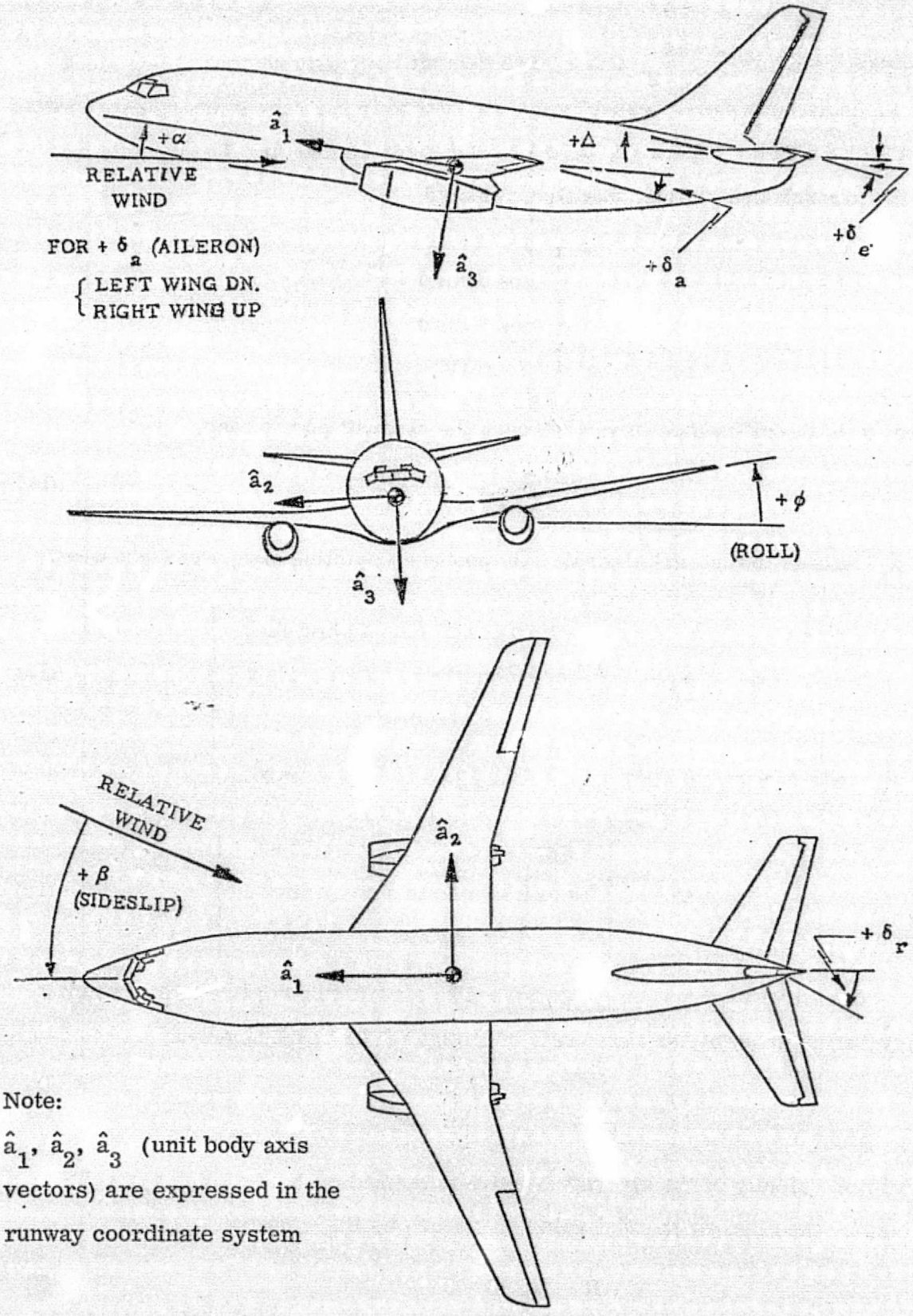

Note:

$\hat{a}_1$, $\hat{a}_2$, $\hat{a}_3$ (unit body axis vectors) are expressed in the runway coordinate system

Figure 2(a). Aircraft Body Coordinate System, Control Surface Deflections, and Aerodynamic Angles.

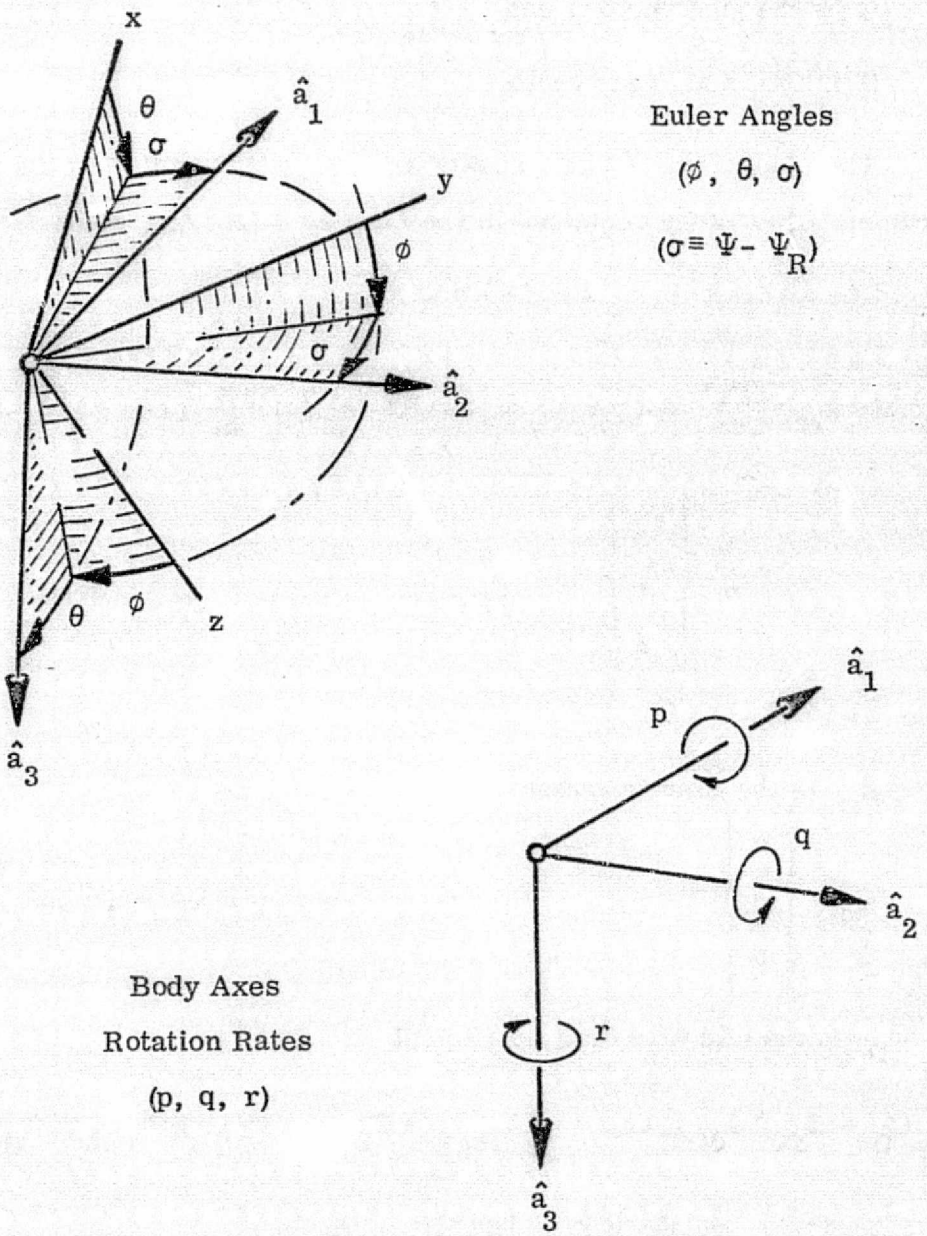

Figure 2(b). Euler Angles and Rotation Rates Defined.

W is the constant wind vector,

G is the gust vector, and

S is the wind shear vector.

The simulation of wind, shears and gust was supplied by the Langley Flight Instrument Laboratory contained in the Langley FLTFAST computer program.

The aircraft linear acceleration is given by,

$$\frac{d^2}{dt^2}R = A_G + \frac{\rho v s}{2m}\left\{-C_D V + C_L(\hat{a}_2 \times V) + C_Y(\hat{a}_3 \times V)\right\} + \frac{k}{m}\left\{\cos\alpha_0\,\hat{a}_1 - \sin\alpha_0\,\hat{a}_3\right\} + \frac{1}{m}\begin{Bmatrix} F_x \\ F_y \\ F_z \end{Bmatrix} \tag{4}$$

where

A_G is the gravity vector

$$A_G = \begin{Bmatrix} 0 \\ 0 \\ G \end{Bmatrix} \tag{4a}$$

C_D is the effective drag coefficient

$$C_D = C_{Do} + C_{D\alpha}(\alpha+\alpha_o) + (C_{Dsp_b} + C_{Dsp_\alpha}(\alpha+\alpha_o))\,\delta_{spb} + C_{D_{GEAR}} + C_{DR}|\delta_R| + C_{D\beta}|\beta| + C_{Dsp}\,\delta_{sp} + C_{D_{G.E.}} \tag{4b}$$

C_L is the effective lift coefficient

$$C_L = C_{Lo} + C_{L\alpha}(\alpha+\alpha_o) + C_{LST}\,\delta_{ST} + C_{Le}\,\delta_e + C_{L_{G.E.}} + C_{Lspb}\,\delta_{spb} + C_{Lsp}\,\delta_{sp} + C_{Lq}\,\frac{\bar{c}}{2v}(q-q_g) + C_{L_{GEAR}} \tag{4c}$$

C_Y is the effective side force coefficient

$$C_Y = C_{Y\beta}\beta + C_{YR}\,\delta_R + C_{Ysp}\,\delta_{sp} + C_{Y\dot{\beta}}\,\frac{\bar{b}}{2v}\,\dot{\beta} + C_{Y\hat{r}}\,\frac{\bar{b}}{2v}\,(r+r_g) \qquad (4d)$$

$$+ C_{Y\hat{p}}\,(p+p_g)\frac{\bar{b}}{2v}$$

The control surface deflections are defined in the notation. The thrust magnitude, k, and the gear forces (F_x, F_y, F_z) will be derived later.

The aerodynamic angles are given by,

$$\alpha = \frac{\hat{a}_3 \cdot V}{\sqrt{(\hat{a}_1 \cdot V)^2 + (\hat{a}_3 \cdot V)^2}}$$

$$\beta = \frac{\hat{a}_2 \cdot V}{v} \qquad (5)$$

The Euler angular velocities of the body are given by the usual kinematic equations (Ref. [1])

$$\dot{\theta} = \cos\varphi\, q - \sin\varphi\, r$$

$$\dot{\psi} = (r\cos\varphi + q\sin\varphi)/\cos\theta \qquad (6)$$

$$\dot{\varphi} = p + \sin\theta\,\dot{\psi}$$

The angular acceleration equations of motion are given by,

$$I_{yy}\dot{q} = (I_{zz} - I_{xx})\,rp + I_{xz}\,(r^2 - p^2) + \frac{1}{2}\rho v^2\, s\bar{c}\, C_M + M_y + k a_T \qquad (7a)$$

$$I_{xx}\dot{p} - I_{xz}\dot{r} = (I_{yy} - I_{zz})\,qr + I_{xz}\,pq + \frac{1}{2}\rho v^2\, s\bar{b}\, C_\ell + M_x \qquad (7b)$$

$$I_{zz}\dot{r} - I_{xz}\dot{p} = (I_{xx} - I_{yy})\,pq - I_{xz}\,qr + \frac{1}{2}\rho v^2\, s\bar{b}\, C_N + M_z \qquad (7c)$$

where C_M is the effective aerodynamic pitching moment coefficient,

$$C_M = C_{Mo} + C_{M\alpha}(\alpha_o + \alpha) + \frac{\bar{c}}{2v} C_{Mq}(q - q_g) + C_{M\,ST}\delta_{ST} + C_{Me}\delta_e + C_{M_{G.E.}}$$

$$+ C_{MR}|\delta_R| + (C_{Mspb} + C_{Mspb\alpha}(\alpha_o + \alpha))\delta_{spb} + \frac{\bar{c}}{2v} C_{M\dot{\alpha}}(\dot{\alpha} - q_g) \tag{7d}$$

$$+ (C_{Msp} + C_{Mspb\alpha}(\alpha_o + \alpha))\delta_{sp} + C_{M\beta}|\beta| + C_{M_{GEAR}} + C_L(.25 - C.G.)$$

C_ℓ is the effective aerodynamic rolling moment coefficient,

$$C_\ell = C_{\ell\beta}\beta + C_{\ell R}\delta_R + C_{\ell a}\delta_a + C_{\ell spb}\delta_{spb} + \frac{\bar{b}}{2v}(C_{\ell p}p_S + C_{\ell r}r_S) \tag{7e}$$

and C_N is the effective aerodynamic yawing moment coefficient,

$$C_N = C_{N\beta}\beta + C_{NR}\delta_R + \frac{\bar{b}}{2v}(C_{Np}p_S + C_{Nr}r_S) + C_{N_{sp}}\delta_{sp} + C_Y\left(\frac{\bar{c}}{\bar{b}}\right)(.25 - C.G.) \tag{7f}$$

$$+ C_{Na}\delta_a$$

(Where p_S and r_S are the roll and yaw in the stability axis system,

$$p_S = \cos\alpha_o\, p + \sin\alpha_o\, r$$

$$r_S = -\sin\alpha_o\, p + \cos\alpha_o\, r \tag{7g}$$

The term $k\,a_T$ is the pitching moment due to thrust.

In order to integrate Equations (7b) and (7c) it is necessary to eliminate the $\frac{d}{dt}r$ term in Equation (7b) and the $\frac{d}{dt}p$ term in Equation (7c). This is accomplished by inverting a 2x2 matrix as follows:

$$\begin{Bmatrix} \frac{d}{dt}p \\ \frac{d}{dt}r \end{Bmatrix} = \frac{1}{I_{xx}I_{zz} - I_{xz}^2} \begin{pmatrix} I_{zz} & I_{xz} \\ I_{xz} & I_{xx} \end{pmatrix} \begin{Bmatrix} I_{xx}\dot{p} - I_{xz}\dot{r} \\ I_{zz}\dot{r} - I_{xz}\dot{p} \end{Bmatrix} \tag{8}$$

The twelve differential equations given by Equations (2), (4), (16), (7a) and (8) are integrated to obtain the required motion of the aircraft. In the simulation a third order Runge Kutta numerical integration scheme, using a time interval of 1/20 second for landing approach and 1/50 second for rollout and turnoff was found to produce accurate results.

(c) Landing Dynamics. The landing gear forces and moments are generated by the ground reaction to the tire and strut deflection and the strut compression rates. In order to compute these deflections and compression rates, it is necessary to describe the relative positions of the tire contact points of the main and nose wheels with reference to aircraft center of mass in the runway inertial system.

The relative coordinates of the three extended, uncompressed gears of the B-737 are given in Reference [2], and shown in Table 2, measured from the leading edge of the mean aerodynamic chord at the aircraft center line in the plane of the MAC. The cartesian coordinates of the ith tire contact point are given by,

$$\begin{aligned} x_{iG} &= x + C.G.\,\bar{c} + \bar{x}_i \\ y_{iG} &= y + \bar{y}_i \\ z_{iG} &= z + \bar{z}_i + \varphi\,\bar{y}_i - \theta\,\bar{x}_i \end{aligned} \tag{9}$$

No gear load or moment can exist until

$$z_{iG} > 0 \tag{10}$$

Since the compression struts are preloaded, no strut deformation can occur until the tire compression load is equal to the ith strut preload. The preload values are given in Reference [2] and illustrated in Figures 3, 4. The landing gear geometry is shown in Figure 5a.

Thus, if

$$0 \leq z_{iG} \leq .0825 \tag{11a}$$

TABLE 1

B-737 AERODYNAMIC COEFFICIENTS AND INERTIAL PARAMETERS

C_{Lo}	= 1.36	C_{Do}	= .185
$C_{L\alpha}$	= 6.9328	$C_{D\alpha}$	= .9225
C_{Lq}	= 8.208	C_{Dspb}	= .0329
C_{LST}	= .963	C_{DLG}	= .07
C_{Le}	= .464	C_{DR}	= -.0258
C_{Lsp}	= -.4584	C_{Dsp}	= .0616
C_{Lspb}	= -.8881	$C_{D\beta}$	= .07
$C_{L_{GEAR}}$	= -.058		
$C_{L\dot{\alpha}}$	= -8.0		
$C_{Y\beta}$	= 1.564	C_{Mo}	= -.155
C_{YR}	= .4383	$C_{M\alpha}$	= -1.4319
C_{Ysp}	= -.06	C_{Mq}	= .0329
$C_{Y\dot{\beta}}$	= 0	C_{MsT}	= -3.437
C_{Yr}	= .189	C_{Me}	= -1.6545
C_{Yp}	= .4871	C_{MR}	= .115
		C_{Mspb}	= .1089
		C_{Msp}	= -.02
		$C_{M\beta}$	= -.34

TABLE 1 (continued)

$C_{\ell\beta}$	=	-.0336	$C_{N\beta}$	=	-.3152
$C_{\ell R}$	=	-.1862	C_{NR}	=	.011
$C_{\ell a}$	=	.011	C_{Na}	=	.0816
$C_{\ell sp}$	=	.0215	C_{Np}	=	.645
$C_{\ell p}$	=	-.2265	C_{Nr}	=	.395
$C_{\ell r}$	=	-.2856	C_{Nsp}	=	.0967

WEIGHT = 90,000 lb.

$\bar{c}$	=	11.2 ft.	I_{xx}	=	375000 lb ft^2
$\bar{b}$	=	93 ft.	I_{yy}	=	875000 lb ft^2
s	=	980 ft^2	I_{xz}	=	480000 lb ft^2
a_T	=	5 ft	I_{zz}	=	1,200,000 lb ft^2

TABLE 2

EXTENDED GEAR LOCATIONS

(Distances in feet from c.g.)

	$\bar{x}$	$\bar{y}$	$\bar{z}$	Gear No.
Right Main Gear	-6.0	8.58	9.78	1
Left Main Gear	-6.0	-8.58	9.78	2
Nose Gear	28.3	0	8.77	3

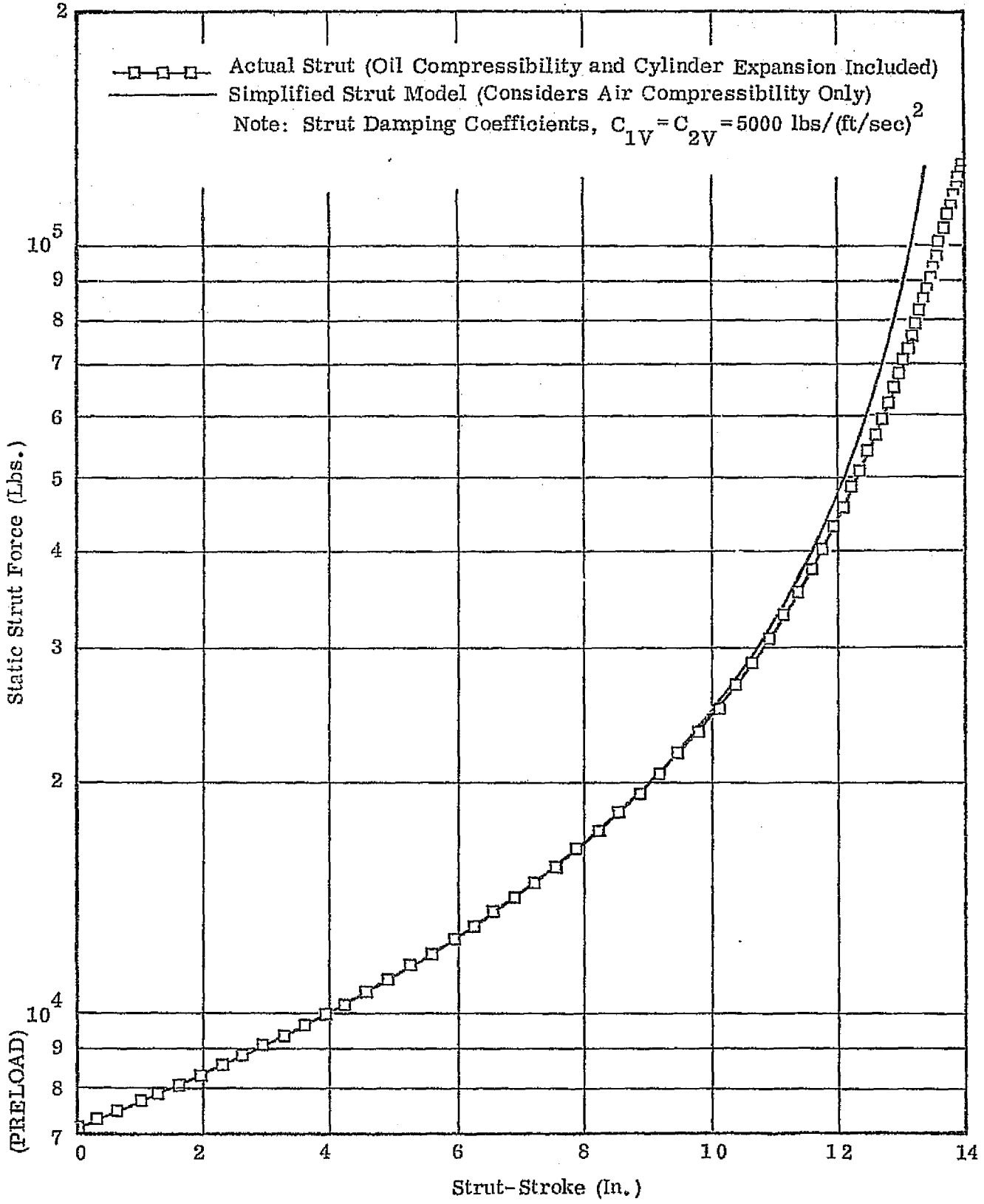

Figure 3. Main Gear Strut Compression Force.

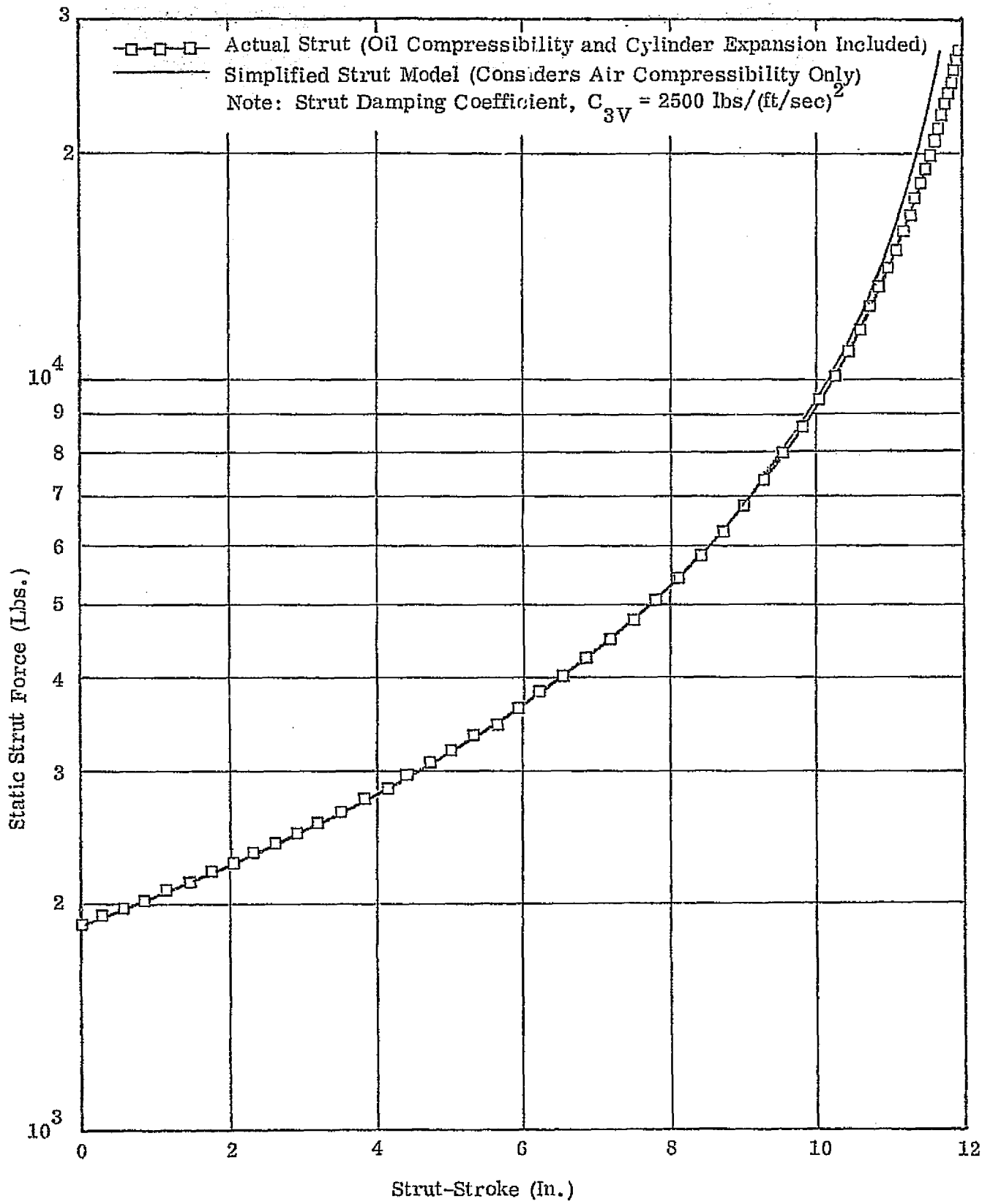

Figure 4. Nose Gear Strut Compression Force.

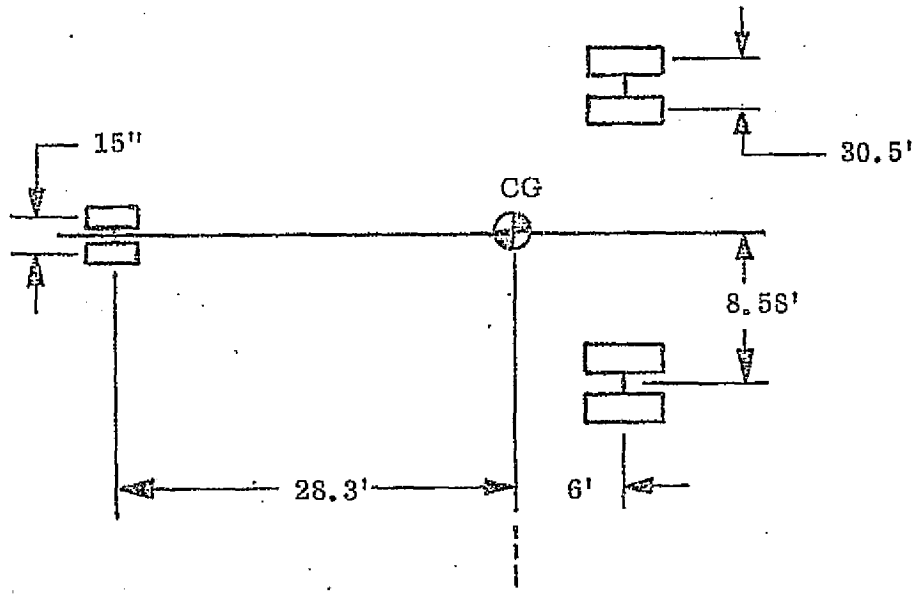

LANDING GEAR LOCATION

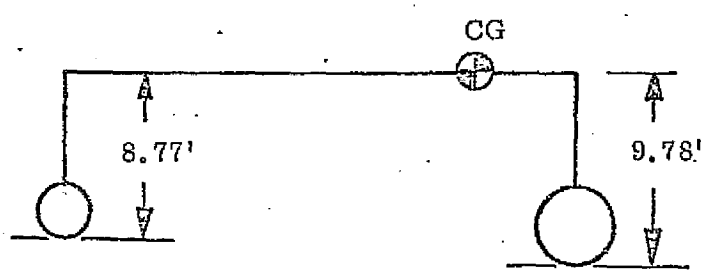

EXTENDED GEAR HEIGHTS

Figure 5(a). Landing Gear Geometry

the strut reaction is a linear function of the tire compression and we have,

$$F_i = - F_{pi} \frac{z_{iG}}{.0825} \tag{11b}$$

Once the preload has been exceeded the strut compression obeys the adiabatic compression law; that is, when

$$.0825 \leq z_{iG} \leq \ell_i$$

we have,

$$F_i = - F_{pi} \left(\frac{1}{1 - \left(\frac{z_i - .0825}{\ell_i} \right)} \right)^{1.4} \tag{11c}$$

To obtain the strut damping force we first compute the strut compression rate $\dot{z}_{Gi}$

$$\dot{z}_{Gi} = (\dot{z} + p\bar{y}_i - q\bar{x}_i) \tag{12}$$

The damping force on the ith strut is given by,

$$F_{Di} = -\dot{z}_{Gi} |\dot{z}_{Gi}| C_{iv} \tag{13}$$

The net strut force, acting normal to the ground, is given by,

$$F_{Ni} = F_i + F_{Di} \tag{14}$$

The tire drag force may now be computed from the tire friction coefficients.

$$F_{Hi} = -\mu |F_{Ni}| \tag{15}$$

The modeling of the tire friction coefficient is taken from References [2 and 3]. For dry runway conditions,

$$\mu = \mu_{ROLLING} + .5 \tag{16}$$

For wet runway conditions,

$$\mu = \mu_{ROLLING} + \frac{V_G + 100}{10V_G + 200} \tag{17}$$

Thus, for high landing speeds and wet runways,

$$\mu \cong \mu_{ROLLING} + .1 \tag{17a}$$

and for taxi speeds (below 20 kts.), and wet runways,

$$\mu \cong \mu_{ROLLING} + .5 \tag{17b}$$

The tire friction curves are shown in Fig. (5b).

Braking for less than the maximum drag coefficient can be achieved by applying partial brake pressure as a control variable. This is developed in the guidance and control sections of the report. Braking is not available on the nose wheel.

The landing gear lateral forces and steering is taken from the theory developed by W.B. Horne in Reference [3]. We first compute the tire compression coefficient η_i:

$$\eta_i = \frac{.5\,|F_{Ni}|}{(p_i + .08\,p_{ri})\,w_i\,(w_i d_i)^{\frac{1}{2}}} \tag{18}$$

If

$$\eta_i > .09$$

the tire compression is given by,

$$\delta_{ti} = w_i\,(.03 + .42\,\eta_i) \tag{19a}$$

If

$$\eta_i < .09$$

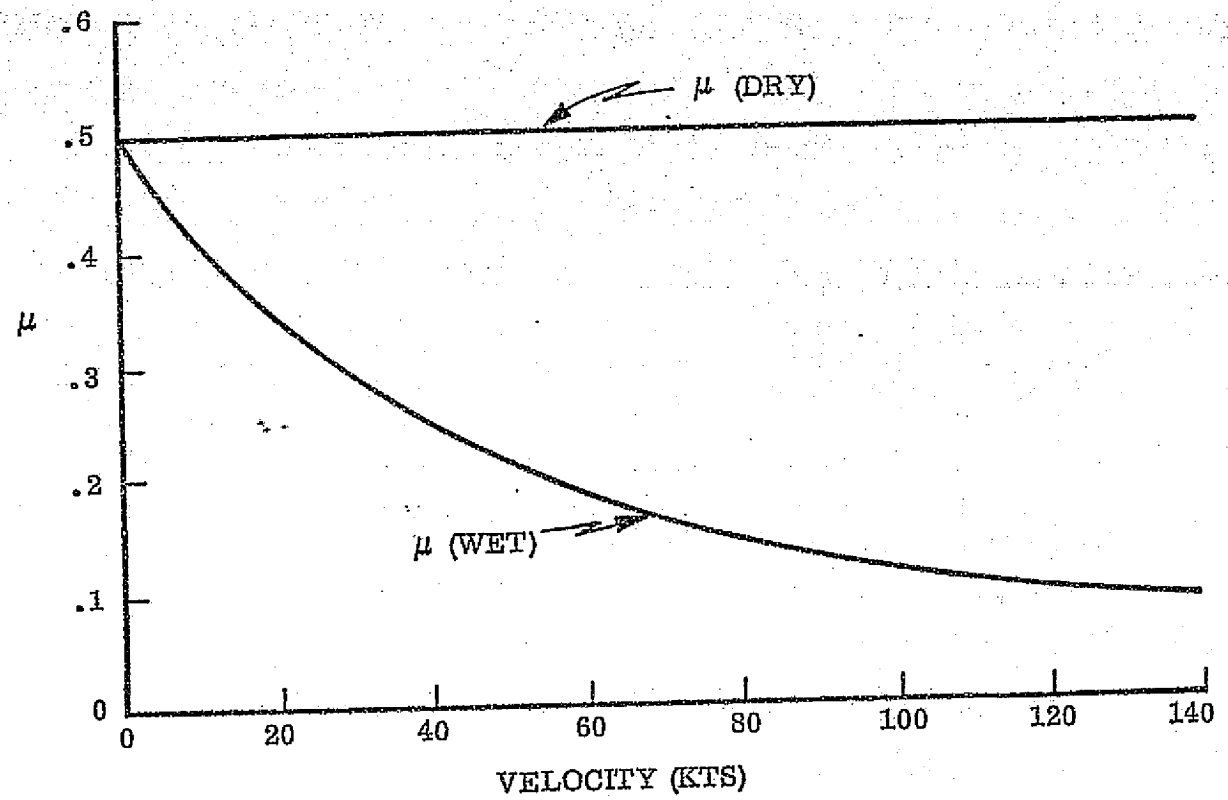

Figure 5(b). Friction Coefficients.

$$\delta_{ti} = \frac{3}{4} w_i \eta_i \tag{19b}$$

The tire cornering force coefficient is given by,

$$C_{Ni} = \frac{2\pi}{180} (p_i + .44\, p_{ri})\, w_i^2 . \tag{20}$$

For

$$\delta_{ti} \geq .0875\, d_i$$

$$N_i = C_{Ni} \left(.067 + .34 \frac{\delta t_i}{d_i}\right) \tag{20a}$$

and for $\delta_{ti} < .0875\, d_i$

$$N_i = C_{Ni} \left(1.2 \frac{\delta_{ti}}{d_i} - 8.8 \left(\frac{\delta_{tI}}{d_i}\right)^2\right) \tag{20b}$$

The lateral tire cornering force is given

$$F_{Li} = N_i (\gamma_i + \sigma - \epsilon_i) \tag{21}$$

where ϵ_i is the ground track angle given by,

$$\epsilon_i = \tan^{-1} \frac{\dot{y} + r(x_{iG} \cos \sigma - \bar{y}_i \sin\sigma)}{\dot{x}} \tag{22}$$

γ_i is the steering angle,

σ is the aircraft yaw relative to the runway yaw.

The landing gear forces, as given above are in the runway system. The net gear forces from the three gears are given by

$$\begin{aligned} F_x &= F_{LS}\, \gamma + \sum_{i=1}^{3} F_{Hi} \\ F_y &= \sum_{i=1}^{3} F_{Li} \\ F_z &= \sum_{i=1}^{3} F_{Ni} \end{aligned} \tag{23}$$

To obtain the landing gear moments in the body system, we have

$$
\begin{aligned}
M_x &= \sum_{i=1}^{3} \left(\left(F_{Hi}\,\theta - F_{Li}\,\varphi + F_{Ni} \right) \bar{y}_i - \left(F_{Li} + F_{Ni}\,\varphi \right) z_{Gi} \right) \\
M_y &= \sum_{i=1}^{3} \left(\left(F_{Hi} - F_{Ni}\,\theta \right) z_{Gi} - \left(F_{Hi}\,\theta - F_{Li}\,\varphi + F_{Ni} \right) x_{Gi} \right) \\
M_z &= \sum_{i=1}^{3} \left(\left(F_{Li} + F_{Ni}\,\varphi \right) x_{Gi} - \left(F_{Hi} - F_{Ni}\,\theta \right) \bar{y}_i \right).
\end{aligned}
\tag{24}
$$

II. NAVIGATION AND FILTERING

This section contains the description of the navigation system. The B-737 is equipped with body mounted accelerometers and rate gyros. Figure 6 contains a block diagram of the functional relationships of the input IMU data, the MLS and radar altimeter measurements and the navigation and filtering functions that are required to feed information to the Autoland guidance and pilot displays.

An optimum utilization of this equipment would require a Kalman type filter that would be capable of estimating MLS biases, winds, etc.

Such a system is outlined in Reference [4], and further study of such a system is highly recommended. However, for the purposes of the study it was found sufficient to utilize a simpler fixed gain complementary filter technique for landing approach, rollout and turnoff. The navigation and complementary filter equations are given in this section.

(a) Navigation. The body mounted accelerometers measure the specific force acting on the aircraft in body system coordinates. To transform the specific force into the runway system it is necessary to obtain the aircraft altitude angles with respect to the runway. These angles are supplied by the aircraft inertial platform unit. Let

$$\begin{aligned} \phi &= \text{roll} \\ \theta &= \text{pitch} \\ \Psi &= \text{yaw (measured from magnetic north)} \\ \Psi_R &= \text{runway yaw (measured from magnetic north)} \end{aligned} \tag{25}$$

Then,

$$T_1(\phi) = \begin{pmatrix} 1 & 0 & 0 \\ 0 & \cos\phi & \sin\phi \\ 0 & -\sin\phi & \cos\phi \end{pmatrix} \tag{26}$$

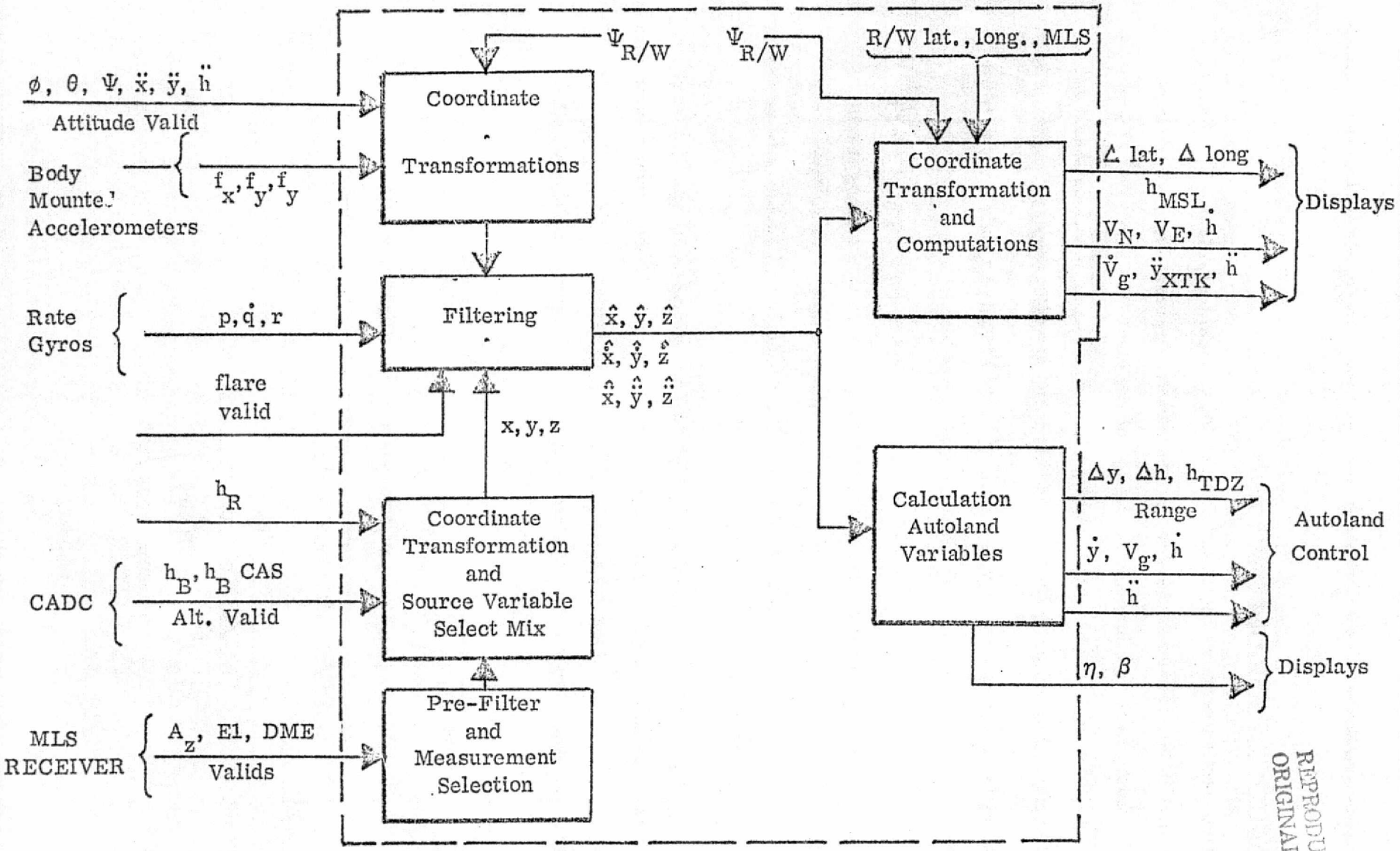

Figure 6. Navigation System Block Diagram

$$T_2(\theta) = \begin{pmatrix} \cos\theta & 0 & -\sin\theta \\ 0 & 1 & 0 \\ \sin\theta & 0 & \cos\theta \end{pmatrix}$$

(26) cont.

$$T_3(\sigma) = \begin{pmatrix} \cos\sigma & \sin\sigma & 0 \\ -\sin\sigma & \cos\sigma & 0 \\ 0 & 0 & 1 \end{pmatrix}$$

where

$$\sigma = \Psi - \Psi_R$$

The dead reckoning estimate of the aircraft acceleration in the runway system is given by,

$$\frac{d^2}{dt^2}\bar{R} = \begin{Bmatrix} 0 \\ 0 \\ G \end{Bmatrix} + T_3(-\sigma)\, T_2(-\theta)\, T_1(-\phi) \begin{Bmatrix} f_x \\ f_y \\ f_z \end{Bmatrix} \tag{27}$$

The complementary filter utilizes this acceleration to produce the estimated aircraft position and velocity by adding a correction proportional to the residual between the MLS measured aircraft position in the runway system and the aircraft estimate of its position.

(b) Complementary Filter. It is not surprising that with a good estimate of the aircraft attitude and acceleration it is possible to integrate the accelerations and obtain a good estimate of the aircraft position and velocity. Under such conditions, the main purpose of navigation aids such as ILS, MLS, etc., is to correct for errors in the IMU due to gyro drift, accelerometer biases, etc. Such a system is outlined in Reference [4] and utilizes a square root version of the Kalman filter with exponential correlated process noise. Such a filter possesses time varying gains and requires considerable skill in design, formulation and execution. The Kalman filter estimates corrections to the integrated IMU aircraft state by optimally minimizing

the covariance matrix of the errors in the aircraft state and the instrument biases. A complementary filter can be designed to provide a similar set of non-varying gains, without any relationship to the uncertainty in the aircraft state or the biases in the IMU and MLS measurements. By adjusting the complementary filter gains to pass the relative low frequency of the true aircraft acceleration it is possible to filter out the high frequency noise in the MLS measurements. The main criterion for such a filter is to provide a stable estimator, one that decays disturbances exponentially and lets the low frequency motions persist. A block diagram of the complementary filter is shown in Figure 7.

Let one of the coordinates of the $\hat{R}(t)$ vector be $\hat{x}_i(t)$. The differential equations of the complementary filter for the x_i coordinate are given by,

$$\begin{aligned}
\frac{d}{dt}\hat{x}_{i1}(t) &= K_1(x_{MLS_i} - \hat{x}_{i1}(t)) + \hat{x}_{i2}(t) \\
\frac{d}{dt}\hat{x}_{i2}(t) &= K_2(x_{MLS_i} - \hat{x}_{i1}(t)) + \hat{x}_{i3}(t) + \ddot{\bar{x}}_i(t) \\
\frac{d}{dt}\hat{x}_{i3}(t) &= K_3(x_{MLS_i} - \hat{x}_{i1}(t))
\end{aligned} \tag{28}$$

where

$\ddot{\bar{x}}_i(t)$ = i component of $\ddot{\bar{R}}(t)$

It is plain that if the residual $x_{MLS_i} - \hat{x}_{i1}(t)$ is zero, the complementary filter will provide the dead reckoning solution of the aircraft motion in the runway system. Moreover, the system is linear with constant coefficients (K_1, K_2 and K_3, the filter gains), with non homogeneous forcing functions due to the noisy MLS measurements and the aircraft estimate of acceleration obtained from the gyros and accelerometers. By choosing the values of K_1, K_2 and K_3, the solution can be designed to be stable and to filter out the high frequency noise.

Since the MLS measurements are available only in a discrete form at fixed intervals (see the next section) and the output of the accelerometers are

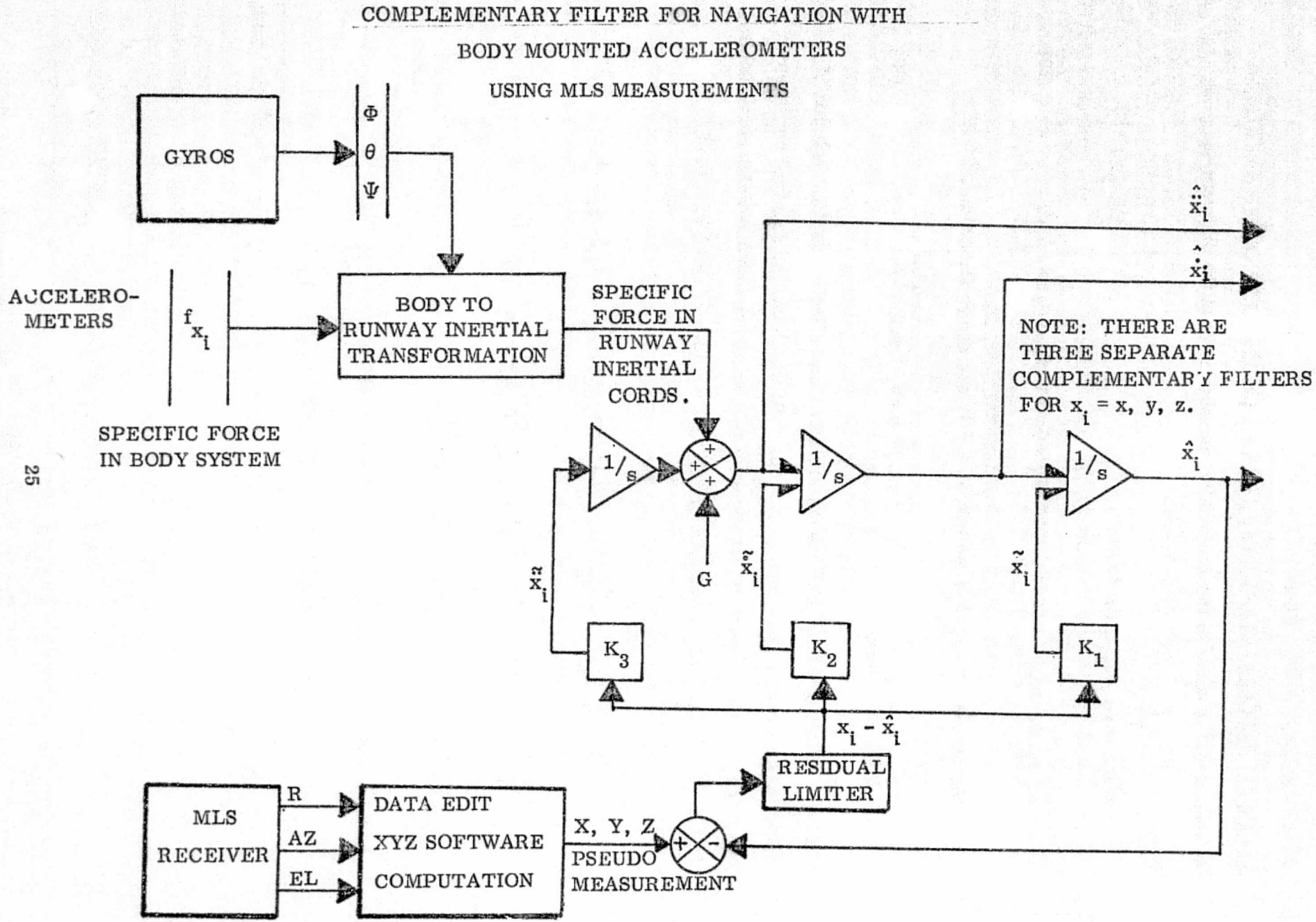

Figure 7. Complementary Filter for Navigation With Body Mounted Accelerometers Using MLS Measurements

available at fixed intervals, we may produce a pseudo MLS measurement which is continuous and is equal to the actual MLS measurement at the discrete sampling time.

We choose $x_{MLS_i}(t)$ to be:

$$x_{MLS_i}(t) = x_{MLS_i}(t_o) + \hat{x}_{i2}(t_o)(t-t_o) + (\ddot{\bar{x}}_i(T) + \hat{x}_{i3}(t_o))(t-t_o)^2/2 \tag{29}$$

We choose $x_{MLS_i}(t_o)$ so that at $t = T$, the observation time,

$$x_{MLS_i}(t_o) = x_{obs_i}(T) - \hat{x}_{i2}(t_o)\,\Delta T - (\ddot{\bar{x}}_i(T) + \hat{x}_{i3}(t_o))\,\frac{\Delta T^2}{2} \tag{30}$$

With this definition of the MLS measurement we can effect an explicit solution of system of differential equations (Equations (28)) which has the required conditions that if the residual is zero we get the dead reckoning solution and which corrects the state to match the MLS observations, without the high frequency component. The solution is given by,

$$\begin{aligned}
\hat{x}_{i1}(T) &= \hat{x}_{i1}(t_o) + \hat{x}_{i2}(t_o)\,\Delta T + (\ddot{\bar{x}}_i(T) + \hat{x}_{i3}(t_o))\frac{\Delta T^2}{2} + b_1\,(x_{MLS_i}(t_o) - x_{i1}(t_o)) \\
\hat{x}_{i2}(T) &= \hat{x}_{i2}(t_o) + (\ddot{\bar{x}}_i(T) + \hat{x}_{i3}(t_o)\,\Delta T + b_2(x_{MLS_i}(t_o) - x_{i1}(t_o)) \\
\hat{x}_{i3}(T) &= \hat{x}_{i3}(t_o) + b_3(x_{MLS_i}(t_o) - x_{i1}(t_o))
\end{aligned} \tag{31}$$

where the constants b_1, b_2 and b_3 are functions of K_1, K_2, K_3 and ΔT.

$$b_1 = \begin{pmatrix} \alpha^2 e^{-\alpha\Delta T} + ((\omega^2+\beta^2) - 2\alpha\beta)\, e^{-\beta\Delta T}\cos(\omega\Delta T) \\ + (\alpha(\beta^2 - \omega^2) - \beta(\beta^2+\omega^2))\, e^{-\beta\Delta T}\sin(\omega\Delta T)/\omega \end{pmatrix} \quad \frac{1}{\alpha^2+\omega^2+\beta^2-2\alpha\beta}$$

$$b_2 = \begin{pmatrix} 2\alpha^2\beta(e^{-\alpha\Delta T} - e^{-\beta\Delta T}\cos(\omega\Delta T)) \\ +(\alpha^2(\beta^2-\omega^2) - (\omega^2+\beta^2)^2)\, e^{-\beta\Delta T}\sin(\omega\Delta T)/\omega \end{pmatrix} \frac{1}{\alpha^2+\omega^2+\beta^2-2\alpha\beta}$$

(32)

$$b_3 = \begin{pmatrix} K_3(\alpha(e^{-\alpha\Delta T} - e^{-\beta\Delta T}\cos(\omega\Delta T)) \\ +(\alpha-\beta)\, e^{-\beta\Delta T}(\sin(\omega\Delta T)/\omega) \end{pmatrix} \frac{1}{\alpha^2+\beta^2+\omega^2-2\alpha\beta}$$

The constants, α, β, ω are the roots of the characteristic equation of the system defined by Equations (28).

$$(S+\alpha)(S+\beta+i\omega)(S+\beta-i\omega) = S^3 + K_1 S^2 + K_2 S + K_3 = 0$$

$$K_1 = \alpha + 2\beta$$

$$K_2 = 2\alpha\beta + \beta^2 + \omega^2 \qquad (33)$$

$$K_3 = \alpha(\beta^2 + \omega^2)$$

By choosing small positive values of α, β, and ω we can obtain a stable low pass filter. We recommend values of

$$\alpha = .08$$

$$\beta = \omega = \frac{\alpha}{\sqrt{2}} \qquad (34)$$

To provide estimates of position, velocity and acceleration for the Autoland equations and display, we have,

$$\hat{x}_i(t) = \hat{x}_{i1}(t)$$
$$\dot{\hat{x}}_i(t) = \hat{x}_{i2}(t) \qquad (35)$$
$$\ddot{\hat{x}}_i(t) = \ddot{\bar{x}}(t)_i + \hat{x}_{i3}(t)$$

III. GUIDANCE

This section describes the equations in the B-737 Autoland guidance system that were used in the simulation study for landing approach. The section also derives a set of guidance equations for rollout and turnoff based on following a buried magnetic cable. The rollout and turnoff guidance will operate using position and velocity information based on MLS measurements. Some question exists whether the range bias can be solved for and eliminated to provide for a safe high speed turn (30-50 ft/sec) in CAT III conditions.

(a) Landing Approach (Airborne) This section describes the guidance equations used in commanding a single banked turn approach from an initial fixed azimuth and aircraft attitude to the runway azimuth at the point at which the aircraft reaches the runway centerline. The guidance consists of a vertical control law, a lateral control law, coupled with automatic throttle control to follow a circular ground track at a desired constant descent flight path angle.

1) Vertical Path Control. The desired vertical descent rate is given by,

$$HDOT_c = -\bar{V}_G \sin(GAMMA) \tag{36}$$

where

$$\bar{V}_G = 120 \text{ KNOTS} \tag{36a}$$

GAMMA = COMMAND FLIGHT PATH ANGLE

The commanded vertical acceleration is zero.

$$HDD_c = 0 \tag{36b}$$

The commanded altitude is

$$H_c(I) = H_c(I-1) + HDOT_c * \Delta T \tag{36c}$$

The vertical guidance equations are given by,

ROLL = ϕ (DEGREES)

QDEG = $\hat{Q}$ (DEGREES/SEC)

HDDOT = $-\ddot{\hat{x}}_3$

HDOT = $-\dot{\hat{x}}_3$

HIGHT = $-\hat{x}_3$

$$\dot{Y}_1 = .16\ (HDOT_c - Y_1), \quad (Y_1(0) = HDOT_c) \tag{37a}$$

$$|\dot{Y}_1| \leq 2.$$

$A = .6\ Y_1$

$B = .09\ (H_c(I) - HIGHT)$

$C = A + B + HDD_c$

$|C| \leq 50.$

IF $(H_c(I) - HIGHT) < 0.$ $f(\alpha) = 1.$

$D = C\,f(\alpha)$, ($f(\alpha)$ IS FIG. 8)

$E = -D + 6.\ HDOT$

$|E| \leq 5.$

$$\dot{Y}_2 = .25\ (E + HDDOT), \quad (Y_2(0) = 0) \tag{37b}$$

IF STABILIZER TRIM IS OPERATIVE

AND $(E + HDDOT) \geq 0.$, THEN

$\dot{Y}_2 = 0.$

$$\dot{Y}_3 = .0625\ (QDEG - Y_3), \quad (Y_3(0) = 0) \tag{37c}$$

$F = .8((E + HDDOT) + Y_2 + 2.16\ (QDEG - Y_3) - .004\,ROLL^2)$

$$\dot{Y}_4 = 16.\ (F - Y_4), \quad (Y_4(0) = 0) \tag{37d}$$

$$|Y_4| \leq 8.^{o}$$

The elevator command to the elevator servo is given by,

$$DELEC = Y_4 \tag{38}$$

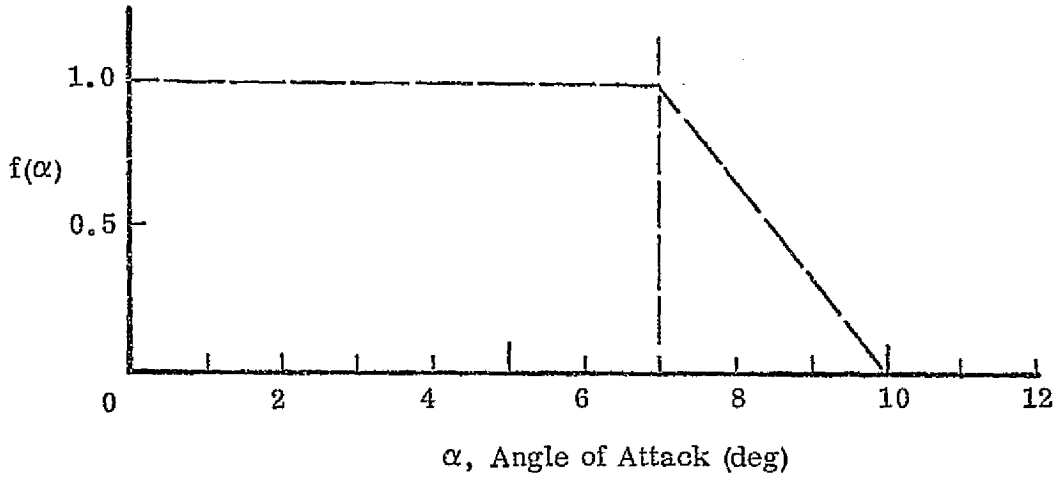

Figure 8. Vertical Path-Angle of Attack Function Control

2) Horizontal Path Control. Let the desired ground path be a circular turn of radius of R_T. The aircraft is assumed to be approaching at a fixed azimuth of Ψ_o. The guidance law produces an aileron deflection designed to keep the aircraft in a constant bank at a fixed airspeed of 120 knots.

Let the aircraft ground track position be $\hat{x}_1$, $\hat{x}_2$ and the turn circle center be W_x, W_y, measured in runway coordinates. The desired yaw is given by,

$$\Psi_D = \tan^{-1} \frac{\hat{x}_1 - W_x}{\hat{x}_2 - W_y} \tag{38a}$$

The cross track error is given by,

$$CRTE = SIGN(W_y)(R_T - \sqrt{(\hat{x}_1 - W_x)^2 + (\hat{x}_2 - W_y)^2}) \tag{38b}$$

The track angle error is given by,

$$TANGE = -\frac{(\hat{x}_1 - W_y)\dot{\hat{x}}_2 + (\hat{x}_1 - W_x)\dot{\hat{x}}_1}{(\hat{x}_1 - W_x)\hat{x}_2 - (\hat{x}_2 - W_y)\hat{x}_1} \tag{38c}$$

The desired bank angle is given in terms of the desired airspeed $\bar{V}_G$

$$\Phi_D = \tan^{-1}\frac{\bar{V}_G^2}{G\,(SIGN\,(W_y)R_T)} \tag{38d}$$

The guidance law bank command is given by,

$$\Phi_c = \Phi_D - C_{YD}(\dot{\hat{x}}_1^2 + \dot{\hat{x}}_2^2)^{\frac{1}{2}}TANGE - C_Y CRTE \tag{39}$$

$$|\Phi_c| \leq 25.^o$$

where

$$C_{YD} = .14$$
$$C_Y = \frac{C_{YD}^2}{7.12} \tag{39a}$$

$$QPOT = .22 + 126.5/AIRSPEED$$

The Autoland guidance equations for the bank angle control is given below:

Let

$$PDEG = \hat{P}(DEGREES/SEC)$$

$$ROLL = \phi\,(DEGREES)$$

$$\dot{Y}_6 = 40.\,(PDEG - Y_6),\quad (Y_6\,(0) = 0) \tag{40a}$$

$$\dot{Y}_5 = 5.\,(\bar{\Phi}_c - Y_5),\quad (Y_5\,(0) = 0) \tag{40b}$$

$$IF\ |5.\,(\bar{\Phi}_c - Y_5)| > 4.$$

replace Equation (40b) by /

$$\dot{Y}_5 = 4. \ (\text{SIGN} \ (\Phi_c - Y_5)) \tag{40c}$$

The aileron command to the aileron servo is given by,

$$\text{DELAC} = 1.82 \ \text{QPOT} \ (Y_5 - Y_6 - \text{ROLL}) \tag{41}$$

$$|\text{DELAC}| \leq 7^{\circ} \tag{41a}$$

A test is made of when to set the desired bank angle to zero. This is done on the displacement from the runway center line.

$$\begin{aligned} &\text{IF} \ |\hat{x}_2| \leq 100. \ \text{FT} \\ &\text{BANKD} = 0. \\ &\text{CRTE} = \hat{x}_2 \\ &\Psi_D = 0. \end{aligned} \tag{42}$$

The guidance equations now return to the AUTOLAND capture mode for a conventional landing. This report does not contain the details of the capture, decrab, and flair logic. These modes were obtained from the Flight Division of Langley Research Center in the form of a computer program called FLTFAST. The simulation of the Auto throttle thrust control, servo control of the stabilizer, elevator, aileron and speed brakes were taken verbatim from the FLTFAST program designed to simulate the AUTOLAND control equations for the B-737.

(b) Landing (Ground Guidance). The landing is divided into three phases, touchdown, rollout and turnoff. During the first phase, as soon as the main gear is preloaded, the throttle is automatically set in idle detent and the speed brakes are automatically engaged. Prior to touchdown this function is inhibited.

For the simulation, a two second linear slowout is employed during which time the ailerons, aileron spoilers, elevator, stabilizer and rudder are brought to zero and the control logic of decrab, flare, etc. is automatically disconnected upon touchdown. The thrust control equations are also disengaged.

For the two second period following touchdown, we have,

$$T_{TD} \leq TIME \leq T_{TD} + 2. \tag{43}$$

$$DELRC(T_D) = \text{RUDDER SERVO COMMAND AT TOUCHDOWN}$$

$$XKK = 1. - \frac{TIME - T_{TD}}{2.} \tag{43a}$$

The rudder servo command is given by a linear mix of DELRC (TD) and the signal provided by the rollout guidance.

$$DELRC = XKK\,(DELRC(TD)) + (1 - XKK)(DELRC(ROLLOUT)) \tag{43b}$$

The guidance logic for the rudder control is given by a feedback of both the error in yaw and the error in yaw rate.

Let the desired yaw, yaw rate, y deviation and lateral velocity be given by

$$RDES = YAWD = YDES = VDES = 0. \tag{44}$$

Let the estimated values of these variables be

$$YAW = \hat{\Psi} \text{ (DEGREES)}$$

$$RDEG = \hat{R} \text{ (DEGREES/sec)}$$

$$YDES = \hat{Y}, \qquad VDES = \dot{\hat{Y}} \tag{44a}$$

The rollout guidance follows:

$$\dot{Y}_1 = 10.\,(RDEG - RDES - Y_1) \qquad (Y_1(0) = 0.) \tag{44b}$$

$$\dot{Y}_2 = 2.5\,(\dot{\hat{Y}} - VDES - Y_2) \qquad (Y_2(0) = 0) \tag{44c}$$

$$ERUD = 7.Y_1 + 4.\,(YAW - YAWD) + 2.\,(.1(\hat{Y} - YDES) + Y_2) \tag{44d}$$

$$|ERUD| \leq 10. \tag{44e}$$

EDAMP = RUDDER DAMPER COMMAND (FROM AUTOLAND EQU.)

$|\text{EDAMP}| \leq 4.$

The rudder command to the servo during rollout is given by,

$$\text{DELRC (ROLLOUT)} = \text{ERUD} + \text{EDAMP} \tag{44f}$$

The speed brakes flaps are brought to a full 40^{o} deflection using a first order servo lag simulation

$$\dot{Y}_2 = 2.(40 - Y_2) \tag{45}$$

The simulation of the thrust to the idle position ($\sim$ 2000.#) is given by a first order servo lag

Let THRUST(ID) be the desired thrust idle, then,

$$\text{THRUST} = e^{-1.\Delta T}(\text{THRUST}-\text{THRUST(ID)}) + \text{THRUST(ID)} \tag{46}$$

(c) Rollout. Rollout begins at the end of the two second slowout. The thrust control is set to maximum reverse thrust (-17,400). Brakes are automatically applied by a law designed to bring the aircraft to a fixed taxi speed. Prior to reaching the taxi speed, when the aircraft reaches a ground speed of 30 knots, the thrust control is commanded to attain a thrust required to balance the drag force at the taxi speed and the rolling friction of the landing gear.

Let

VTAXI = desired taxi-speed

$$V_G = (\hat{\dot{x}}_1^2 + \hat{\dot{x}}_2^2)^{\frac{1}{2}}$$

$$\text{THRUSTC(TAXI)} = C_D \frac{1}{2}\rho(\text{VTAXI})^2 s + .015\ \text{WEIGHT} \tag{47}$$

Thus, when the aircraft speed reaches 30 knots, the thrust is given by,

$$\text{THRUST} = e^{-.6\Delta T}(\text{THRUST}-\text{THRUSTC(TAXI)}) + \text{THRUSTC(TAXI)} \tag{48}$$

The braking logic is given as follows:

$$DLV = VTAXI - VG$$
$$DTVG = (\ddot{\hat{x}}_1 \dot{\hat{x}}_1 + \ddot{\hat{x}}_2 \dot{\hat{x}}_2)/VG \tag{49a}$$

$$ACCDES = (VG + VTAXI)\, DLV/150 - (DTVG - .015\ G)$$

Since the automatic skid device controls the brake pressure to prevent skidding we may simulate the brake pressure by modifying the effective coefficient of friction of the main gear.

$$\text{IF } ACCDES \leq 0 \tag{50a}$$
$$DMUD = 0. \qquad \text{(BRAKE COMMAND ZERO)}$$

$$\text{IF } ACCDES > 0$$
$$DMUD = ACCDES/G \tag{50b}$$
$$YMUD = e^{-2.\Delta T}(YMUD - DMUD) + DMUD \tag{50c}$$
$$|YMUD| \leq .5$$

The coefficient of friction, simulating brake pressure, is now given by

$$\mu = \mu_{ROLLING} + YMUD \qquad \text{(for dry runways)} \tag{50d}$$

and

$$\mu = \mu_{ROLLING} + \frac{VG + 100\ YMUD}{10VG + 200\ YMUD} \qquad \text{(for wet runways)} \tag{50e}$$

(d) Turnoff. The mechanism for providing steering information in this study is a single underground magnetic cable. The design and characteristics are taken from Reference [5]. In this section we derive the guidance law. Steering forces and moments are provided by the nose wheel as indicated in the earlier sections. For automatic control, the nose wheel is locked into a fixed turning ratio to the rudder servo as soon as the nose wheel vertical load exceeds the nose wheel preload. At the high landing speeds when the rudder is still effective, the nose wheel forces are not significant. As the aircraft reaches taxi and turning speeds, the rudder loses its aerodynamic effectiveness and the nose wheel becomes the dominant steering mechanism. The ratio of the nose wheel rotation to rudder rotation on the B-737 is given by,

$$\gamma(\text{DEGREES}) = -\frac{7}{26}\,\delta_R\,(\text{DEGREES}) \tag{51}$$

The guidance law for turnoff uses the same gain constants as for the rollout. The estimates of the errors in yaw and yaw rate are provided by different equations.

A turn is a circular arc of a fixed radius. For the study the radius was taken to be

$$R_T = 120.\ \text{ft} \tag{52}$$

As the aircraft approaches the start of the turnoff, a radio signal indicates the approach of the turn initiation and actuates the turn control circuit.

Let the aircraft position at the start of the turn be $\hat{x}_1(t_s)$, then the center of the turn circle is

$$\begin{aligned} W_x &= \hat{x}_1(t_s) \\ W_y &= R_T * \text{SIGN} \end{aligned} \tag{53}$$

The sign of the turn (to the right or left) is transmitted by a polarity code with the initiation signal.

The magnetic cable yields a signal proportional to the error in yaw and the error in lateral deviation. In order to supply the information for the desired yaw rate and desired lateral deflection rate error, the information is generated from the assumption of a circular turn.

For a turn of fixed radius, the desired yaw rate is given by

$$\text{RDES} = \frac{VG(180)}{R_T\,\pi} * (\text{SIGN}) \tag{53a}$$

To obtain a signal proportional to the track angle error we proceed as follows:

$$XS = \hat{X}_1 - \hat{X}_1(t_s)$$

$$YS = \hat{Y} - SIGN * R_T \tag{53b}$$

$$DRW = \sqrt{XS^2 + YS^2}$$

The error in deviation rate is given by

$$(\dot{Y} - VDES) = -(XS * \dot{\hat{X}}_1 + YS * \dot{\hat{X}}_2) * \frac{SIGN}{DRW} \tag{54}$$

The turnoff guidance law follows the guidance logic given in Eq. (44a) to (44f).

Reference [6] describes a steering law designed for the CV-880, which uses a position error system. Insufficient studies were carried out to determine the advantage or disadvantage of the two laws. More studies are necessary before a firm recommendation can be made.

Once the turn has been completed and the aircraft has a new heading, the guidance law returns to the straight line mode. The logic to initiate the new phase is a radio signal at the start of the straight line segment. The aircraft is given the x_1 and x_2 position and the yaw heading of the start of the center line of the taxi strip as a fixed code input.

The desired yaw is now

$$\Psi_D = \Psi_{RUNWAY} \tag{55a}$$

The desired yaw rate is

$$RDES = 0. \tag{55b}$$

IV. THE MLS OBSERVABLES

The characteristics of the MLS observables are described in documents supplied by Langley Research Center in Reference [7]. The system used is for conical coordinates of aximuth (β), elevation (α) and range. The range and aximuth origin is at the center of azimuth antenna facing outward toward the approaching aircraft along the runway centerline. The elevation origin is offset from the runway and is at the center of the elevation antenna. Thus, the cartesian coordinate system for the MLS observable is the negative of the runway inertial system in the x and z direction and in the same direction as the y of the runway. We have, in the runway coordinate system,

$$\begin{bmatrix} x \\ y \\ z \end{bmatrix}_{MLS} = - \begin{bmatrix} x \\ -y \\ z \end{bmatrix}_{RUNWAY} + \begin{bmatrix} x \\ -y \\ z \end{bmatrix}_{ANTENNA} \tag{56}$$

The origin of the MLS system is at the azimuth antenna and the position of the elevation antenna is measured relative to it. See Figure 9(a).

Let the MLS coordinates of the aircraft be X_M, Y_M, Z_M. Then the observables in the MLS coordinate system are

$$\begin{aligned} \text{RANGE} &= \sqrt{X_M^2 + Y_M^2 + Z_M^2} \\ \beta &= \sin^{-1}(-Y_M/\text{RANGE}) \\ \alpha &= \sin^{-1} \frac{Z_M}{\sqrt{(X_M - X_{EO})^2 + (Y_M - Y_{EO})^2 + Z_M^2}} \end{aligned} \tag{57}$$

In the above, the z coordinate of the elevation antenna is assumed to be at the same altitude as the azimuth antenna, and X_{OE} and Y_{OE} are the coordinates of the elevation antenna from the azimuth origin, in the MLS system.

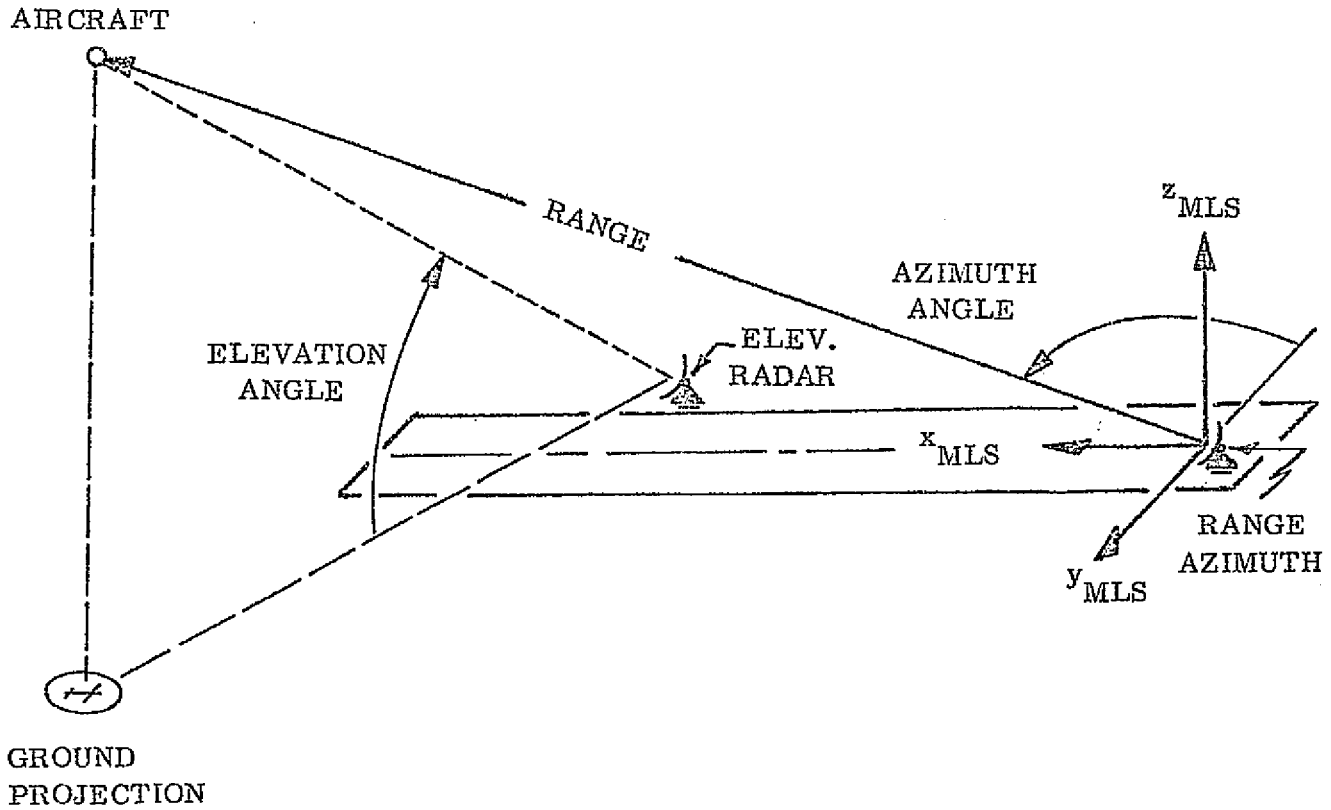

Figure 9(a). The MLS Coordinate System.

To invert the solution and obtain X_M, Y_M, Z_M from range, β and α, we have

$$X_M = g + \sqrt{g^2 - h}$$

$$Y_M = -\text{RANGE}\ (\sin\beta) \tag{58}$$

$$Z_M = \sqrt{(\text{RANGE})^2 - X_M^2 - Y_M^2}$$

where

$$g = X_{OE}\ (\sin\alpha)^2$$

$$h = (X_{OE}^2 + Y_{OE}^2)(\sin\alpha)^2 + Y_M^2 - (\text{RANGE})^2(\cos\alpha)^2$$

$$- 2\,Y_M\,Y_{OE}\,(\sin\alpha)^2$$

Finally, to obtain the aircraft coordinates in the runway inertial system, we have,

$$\begin{bmatrix} x \\ y \\ z \end{bmatrix}_{\text{RUNWAY}} = \begin{bmatrix} x \\ y \\ z \end{bmatrix}_{\text{AZIMUTH ANT}} - \begin{bmatrix} x_M \\ -y_M \\ z_M \end{bmatrix} \tag{59}$$

The noise characteristics are obtained from Reference [7].

For the exponential correlated noise in range, β and α, we have

$$\eta_{EL}(t) = \sigma_{EL}\sqrt{1 - A_{EL}^2}\ u(t) + A_{EL}\,\eta_{EL}(t-1)$$

$$\eta_{AZ}(t) = \sigma_{AZ}\sqrt{1 - A_{AZ}^2}\ u(t) + A_{AZ}\,\eta_{AZ}(t-1) \tag{60}$$

$$\eta_R(t) = \sigma_R\sqrt{1 - A_R^2}\ u(t) + A_R\,\eta_{AZ}(t-1)$$

where u(t) is a random number of zero mean, σ_i is the standard deviation of the ith measurement and

$$A_i = e^{-\frac{\Delta T}{T_i}} \tag{61a}$$

For initialization

$$\eta_i(0) = u(0) \tag{61b}$$

Table 3 contains the values of the noise characteristics used in the MLS error model.

To simulate data dropout, we use a random number with uniform distribution from -1 to 1 and set the observation equal to zero whenever the random number exceeds .98. Thus, 2 percent of each observation string is lost. Since there are three observation types, 6% of the pseudo state observations are lost. This percentage can be varied.

To simulate bad data, a similar random number with a uniform distribution is used, and an average percentage of the observations is set equal to a large number (1000 times the bias) even though the date valid flag is set true. Thus bad data enters the system marked good a small percentage of the time.

Biases are included in the simulation. Values of the biases are initially chosen from a random number generator and retained for the simulation run. The bias values are also given in Table 3.

MLS "jitter" or "stagger" is simulated to produce the data train sequence as shown on Figure 9d.

To accommodate data dropout, MLS invalids and bad data generally, the recommended course of action is to replace the bad data type by the aircraft estimate of the data missing (or considered rejectable) by the best estimate of the data type based on the current values of the vehicle state. Thus, if data is missing, we replace the bad data by range, azimuth or elevation from Eq. (57), using $\hat{X}_M$, $\hat{Y}_M$ and $\hat{Z}_M$ computed from Eq. (56). This mode is still under study.

TABLE 3

MLS ERROR MODELS

Function	Model	A	$\alpha(\frac{1}{sec})$	Γ	u(n)
Elevation	$y(n) = \Gamma\sqrt{1 - A^2}\ u(n) + Ay(n-1)$	$e^{-\alpha T}$	19.100	7.01×10^{-2} Deg.	IGRS
Azimuth	$y(n) = \Gamma\sqrt{1 - A^2}\ u(n) + Ay(n-1)$	$e^{-\alpha T}$	0.971	5.10×10^{-3} Deg.	IGRS
Range	$y(n) = \Gamma\sqrt{1 - A^2}\ u(n) + Ay(n-1)$	$e^{-\alpha T}$	1.013	21.1 Ft.	IGRS

Note: IGRS = Independent Gaussian Random Sample

Initialization is achieved by setting y(0) = u(0).

See Figures 9(b) and 9(c) for illustrations of MLS jitter in azimuth and elevation.

See Figures 10(a), 10 (b), 10 (c) for illustrations of the correlated noise in MLS jitter in azimuth and elevation.

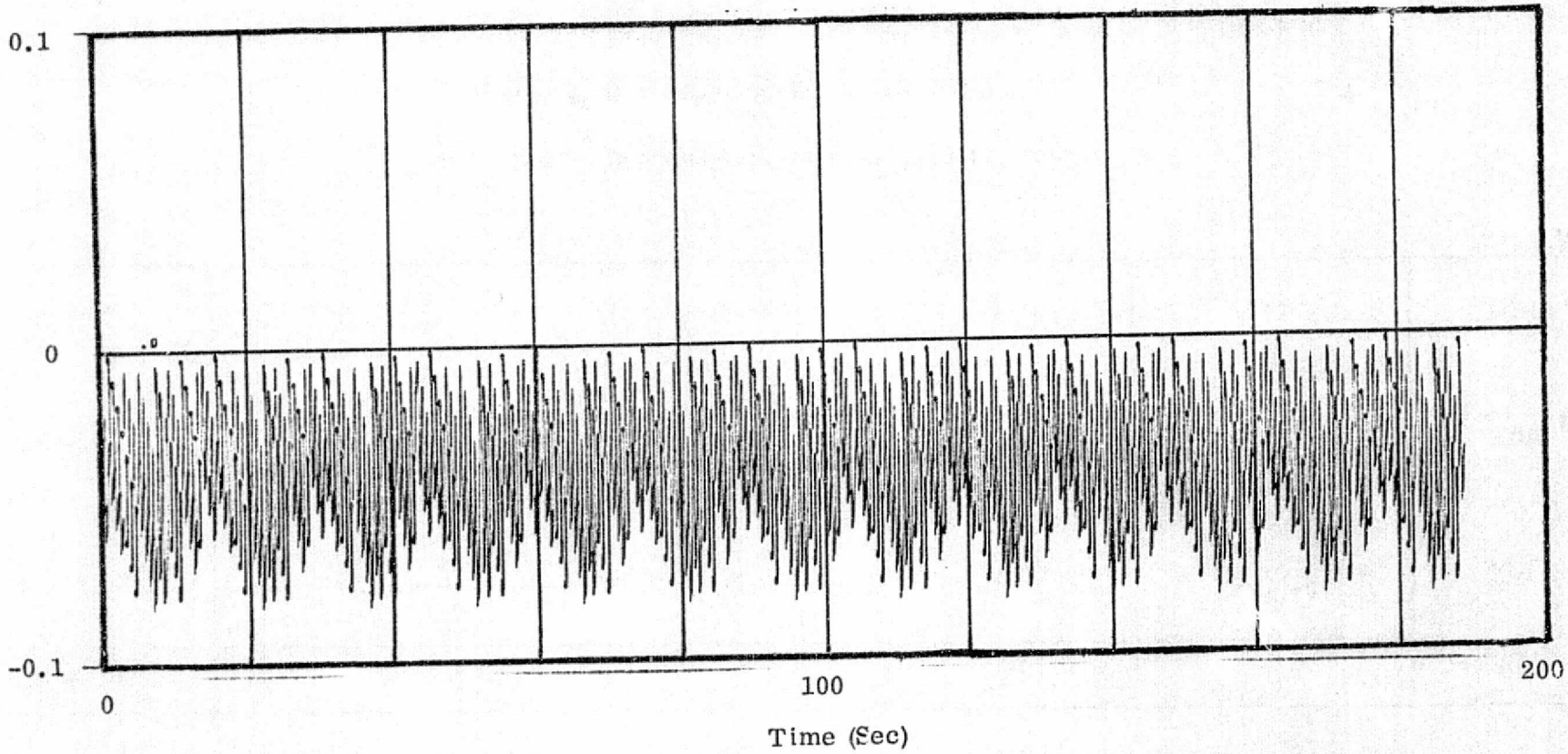

Figure 9(b). MLS Jitter, Azimuth

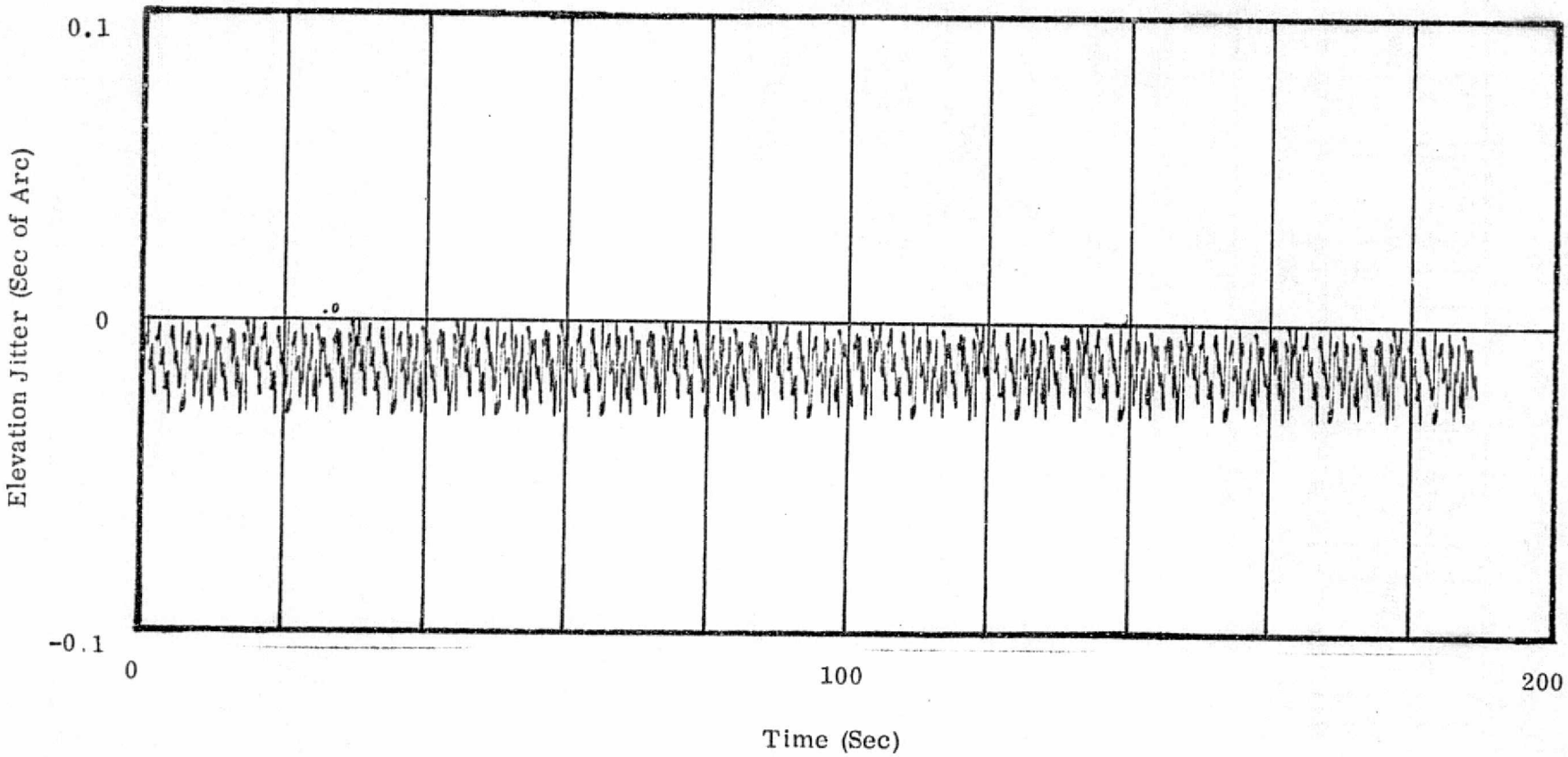

Figure 9(c). MLS Jitter, Elevation

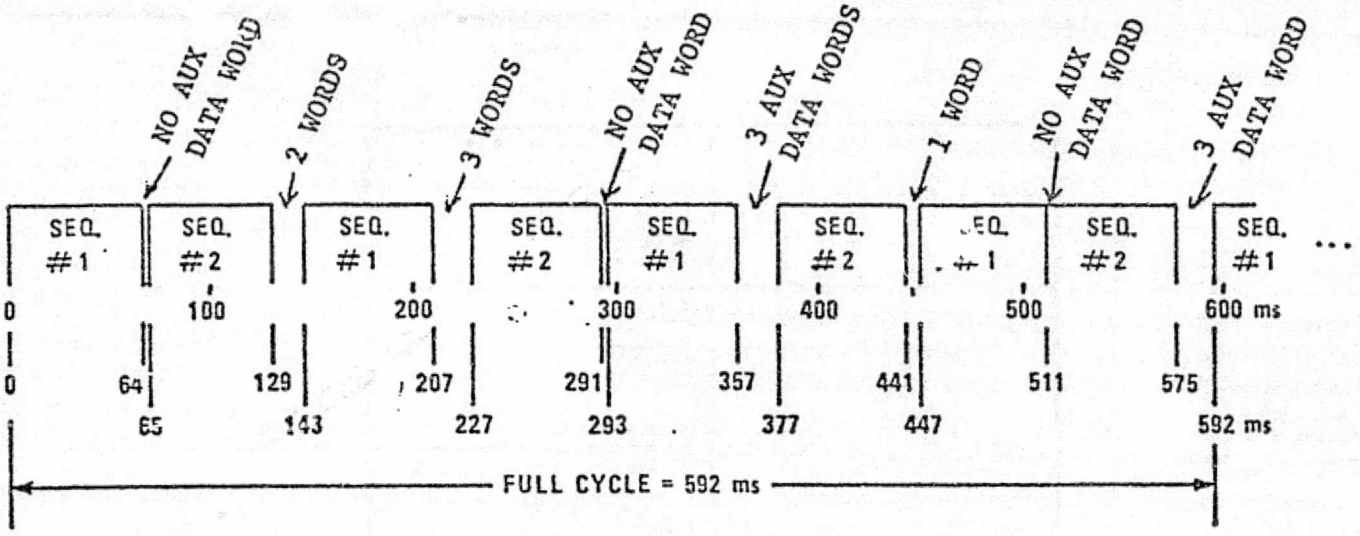

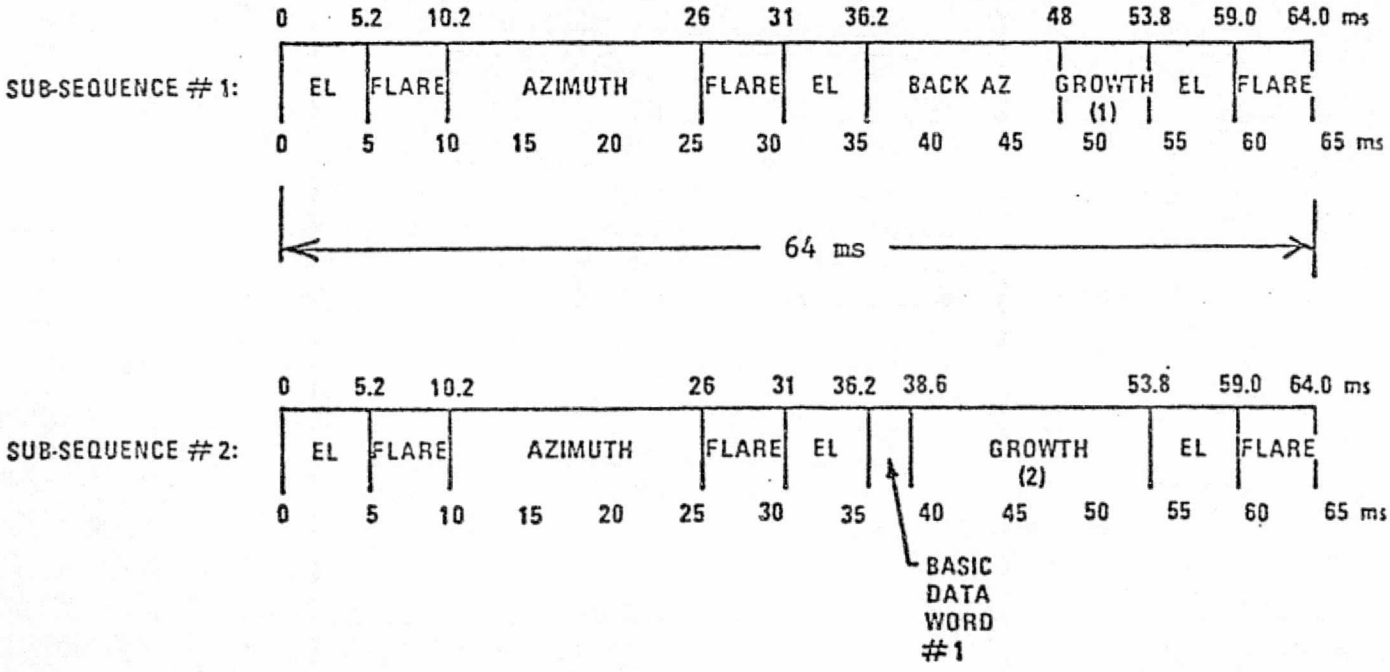

NOTES: (1) AUXILIARY DATA (1 WORD) OR BACK ELEVATION
(2) 360° AZIMUTH

Figure 9(d). Time Sequence for Conical MLS.

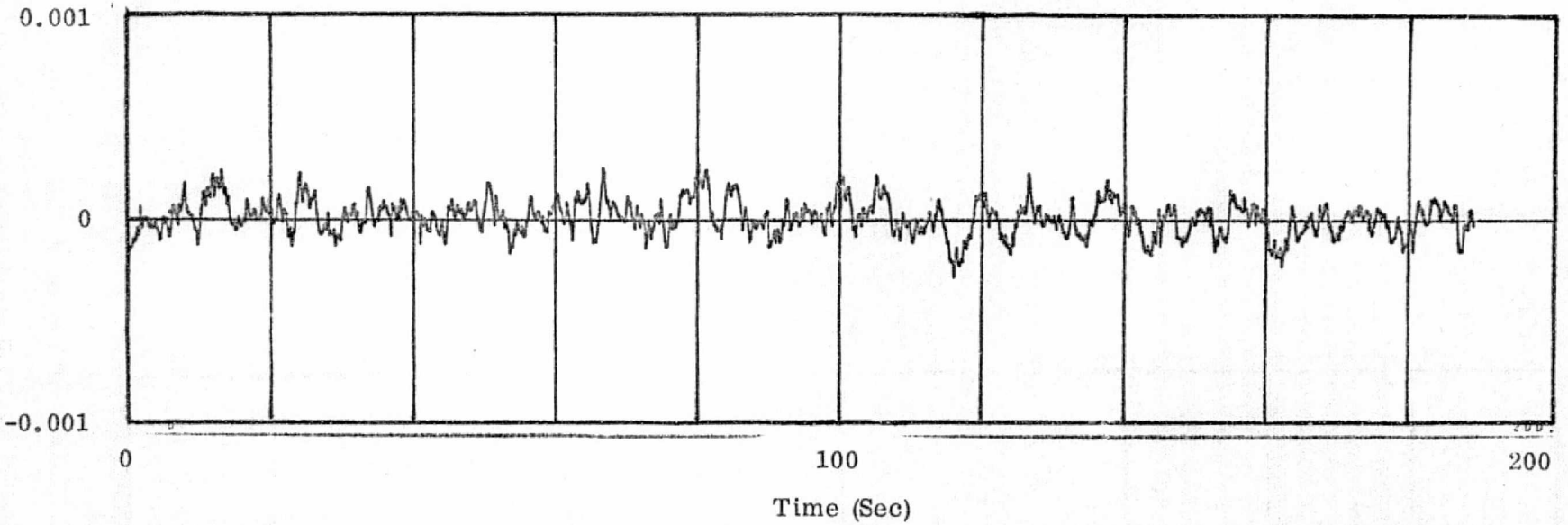

Figure 10(a). Simulated Azimuth Correlated Noise.

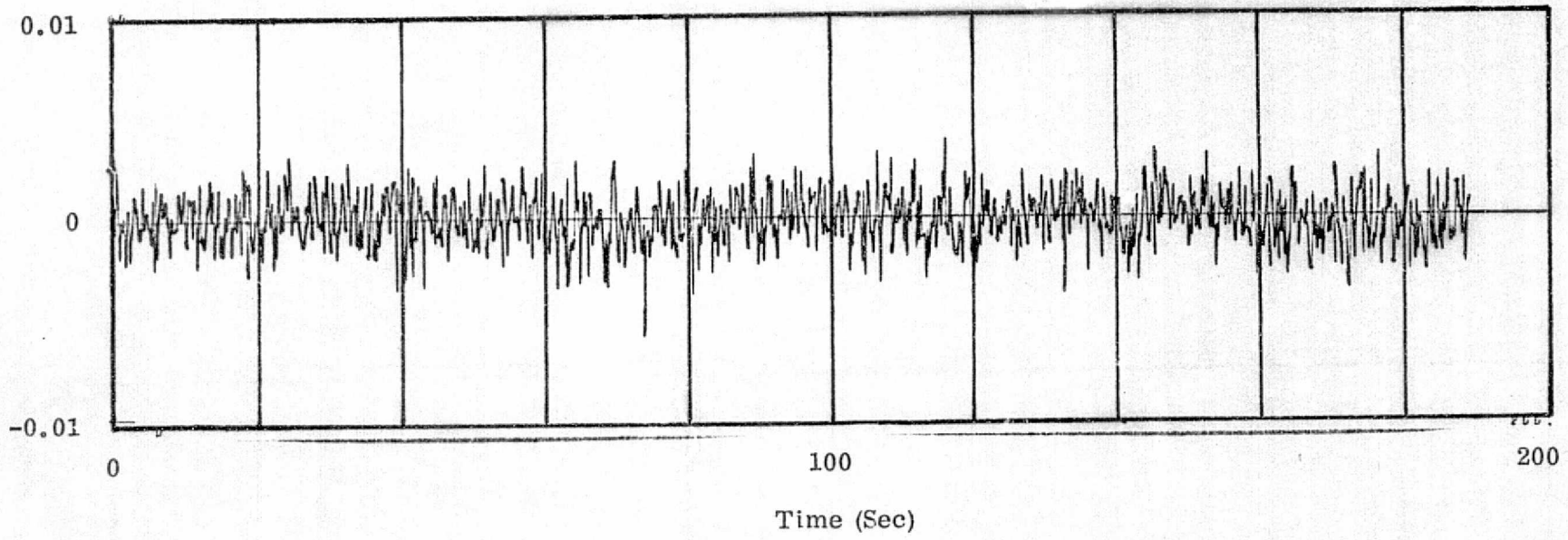

Figure 10 (b). Simulated Elevation Correlated Noise.

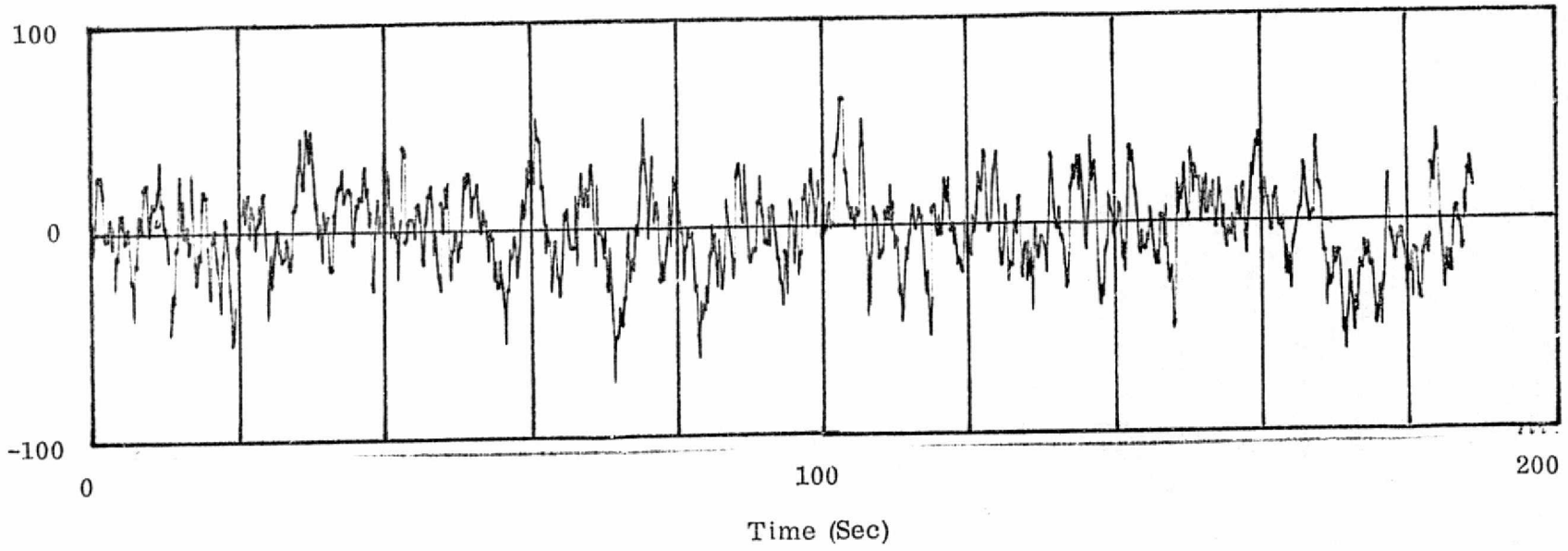

Figure 10(c) Simulated Range Correlated Noise

V. MAGNETIC LEADER CABLE

A single underground magnetic leader cable, as described in Reference [5], is a centerline guide for prescribing the aircraft turn. The system is capable of generating a signal proportional to the distance from the cable centerline and a signal proportional to the yaw error from the cable centerline yaw. These are generated by functions of three voltages (Figure 11).

$$\text{CRTE} = K_1 \frac{v_1}{v_1^2 + v_2^2 + v_3^2}$$

$$\text{TANGE} = K_2 \frac{v_3}{v_2} \quad . \tag{62a}$$

The sign of the heading can be obtained from the phase between v_2 and v_3.

The guidance law for the turn is similar to the rollout with the following changes:

$$\text{RDES} - \text{RDEG} = K_3 \frac{\dot{v}_3 v_2 - \dot{v}_2 v_3}{v_2^2} \tag{62b}$$

$$\text{YAWD} - \text{YAW} = K_2 \frac{v_3}{v_2} \quad . \tag{62c}$$

Finally, the rudder damper signal input to the rudder servo is shut off when the aircraft reaches the turn corner. The gain constants of the rudder-nose wheel guidance law are retained.

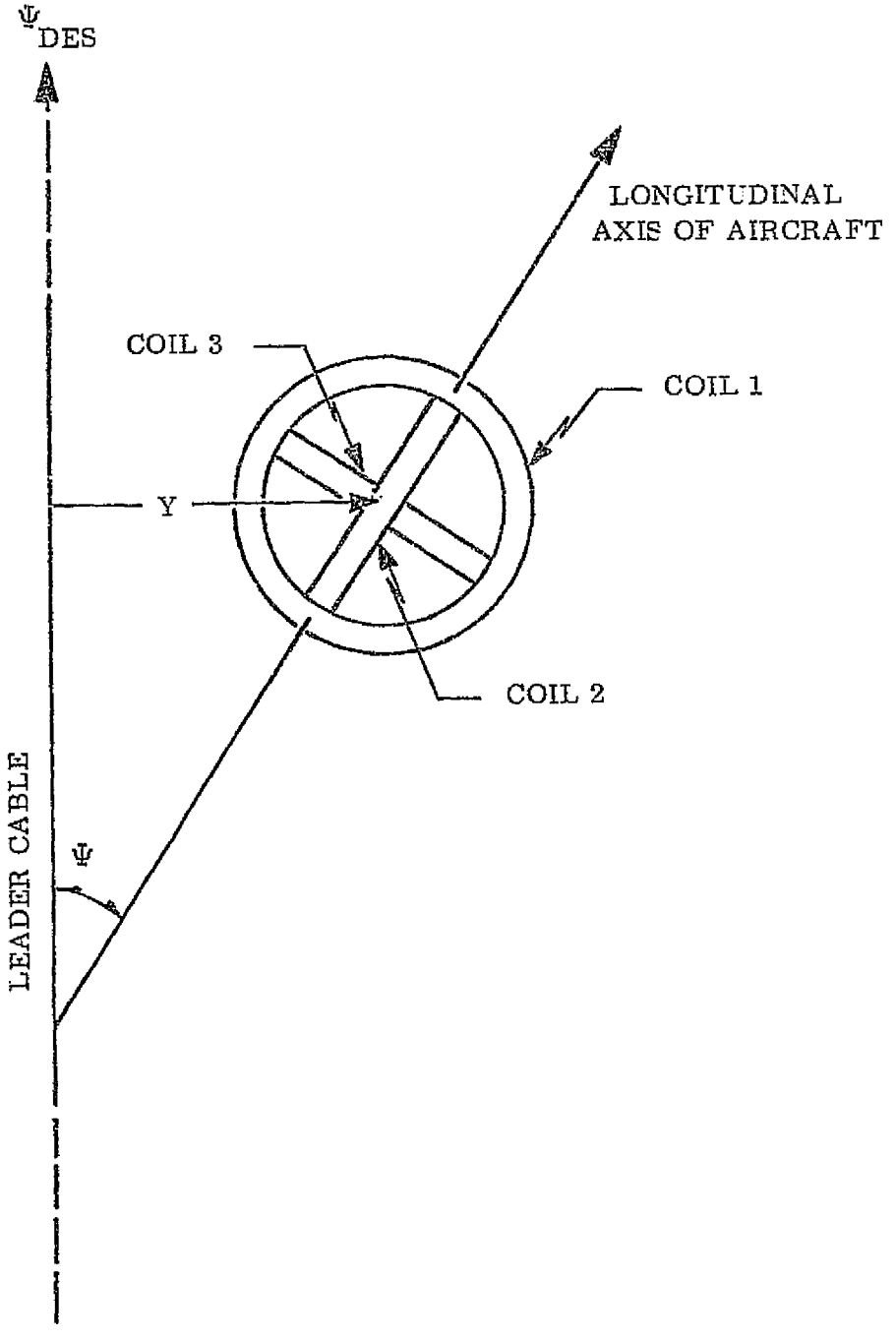

Figure 11. Magnetic Leader Voltage Signals.

VI. PRELIMINARY SIMULATION RESULTS

This section contains a discussion of some of the preliminary results of the simulation program generated using the models outlined in this report.

The airborne guidance using MLS and the complementary filter successfully lands in the aircraft after executing a banked turn from a 165^{o} yaw deviation from the runway with and without winds and gusts. Figures 12(a), 12(b), 12(c), 12(d) and 12(e) are plots of a typical landing showing altitude, descent rate, pitch angle, runway centerline offset and ground speed, versus time for capture, decrab, flair, touchdown, rollout and turnoff.

The results indicate that the MLS system can be used for landing approach in mixed weather conditions. Additional studies, using the simulation program, should be carried out. The rollout and turnoff study shows that the aircraft can be automatically and rapidly decelerated to turnoff speeds using reverse thrust and braking. The magnetic cable concept shows promise as a guidance tool aid. However, here also, additional studies must be carried out before concrete recommendations can be made.

It is recommended that the simulation program described in this report be refined to include a more accurate aerodynamic, landing gear and Autoland guidance model. Further, it is recommended that a noise model be included in the magnetic leader cable simulation. Finally, it is recommended that the competing rollout and turnoff guidance laws be studied so that a CAT III automated rollout and turnoff policy can be finalized for the B-737.

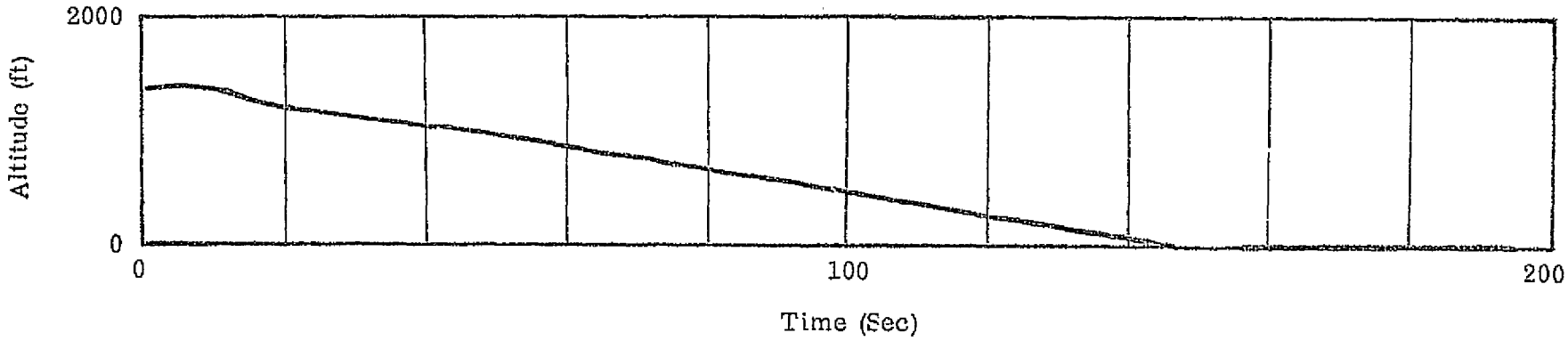

Figure 12(a). Typical Landing Simulation Data, Altitude

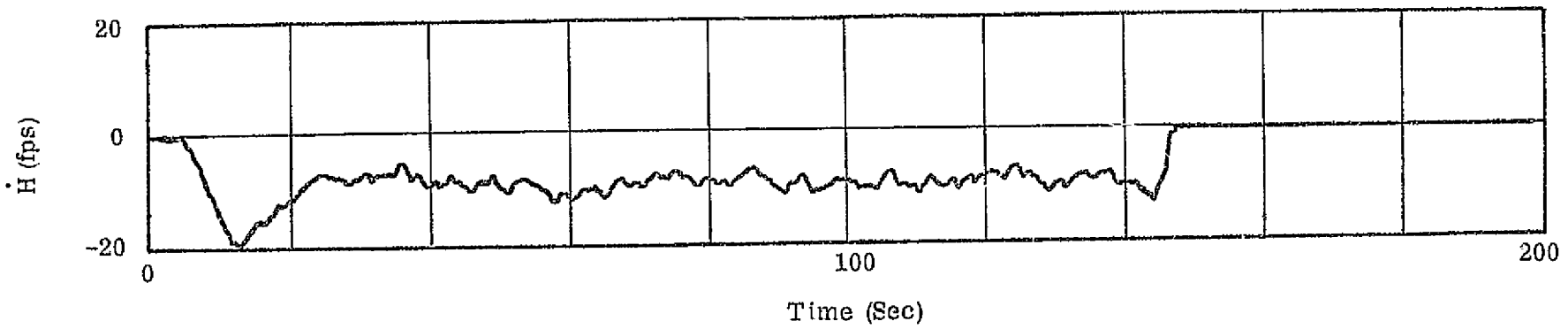

Figure 12(b). Typical Landing Simulation Data, Descent Rate

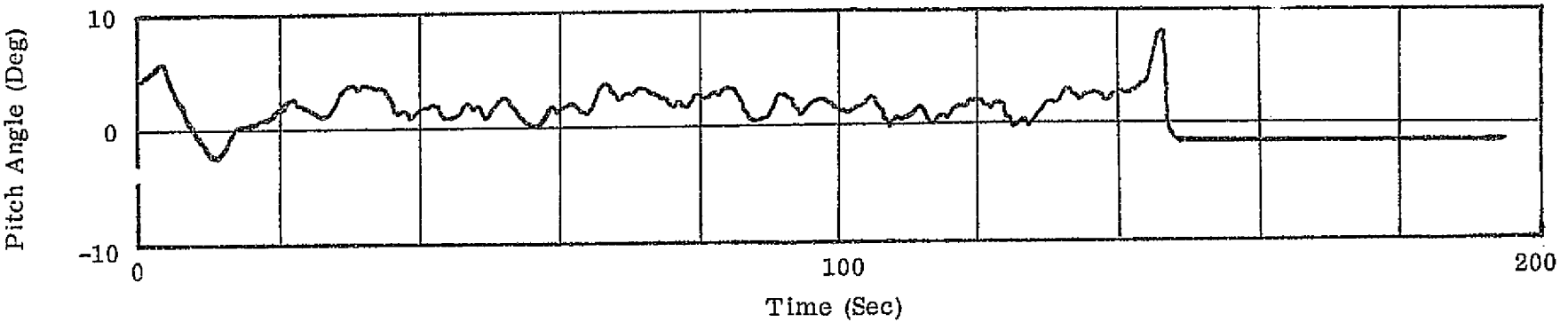

Figure 12(c). Typical Landing Simulation Data, Pitch Angle

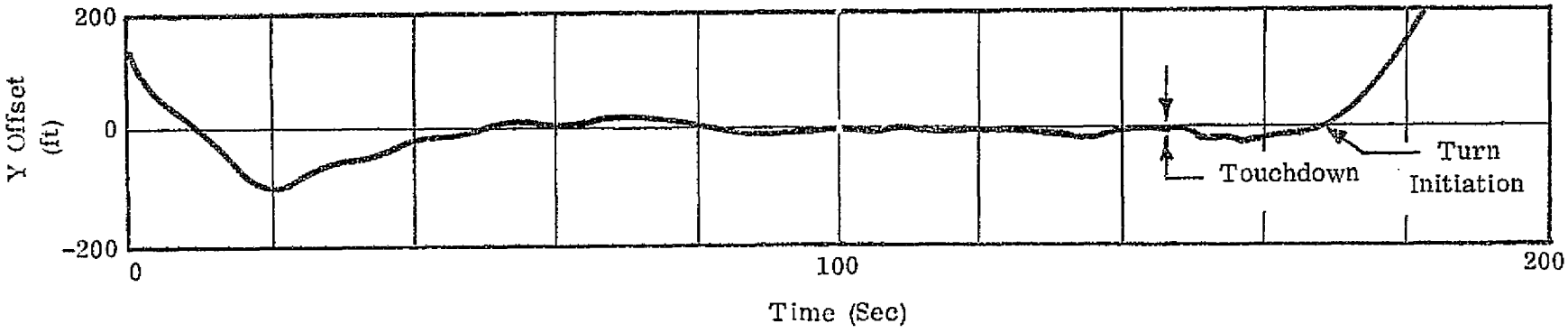

Figure 12(d). Typical Landing Simulation Data, Runway Centerline Offset

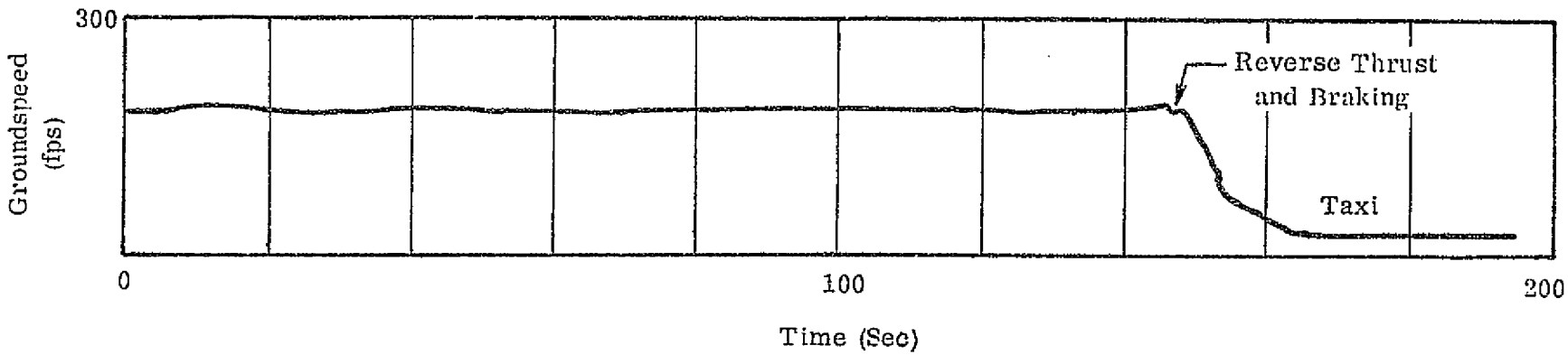

Figure 12(e). Typical Landing Simulation Data, Ground Speed.

REFERENCES

[1] Etkin, B., "Dynamics of Flight", J. Wiley & Sons, New York, 1967.

[2] Attri, N. S., Dunn, R., "NASA Request for Data in Landing Gear, Tires, Antiskid, Thrust, Nose Wheel Dynamics and Rudder Aerodynamics", Boeing Document B-8190-75-5, March 25, 1975.

[3] Horne, W.B. and Leland, T.J.W., "Influence of Tire Tread Pattern and Runway Surface Conditions on Braking Friction and Rolling Resistance of a Modern Aircraft Tire", NASA TN D-1376, 1962.

[4] Schmidt, S.F., "A Conceptual Navigation System for Curved Descending-Decelerating Approaches", AMA Report No. 75-1, January 1975.

[5] Morgan, H.C., England, P., "A Taxi Guidance System for Aircraft using a Single Magnetic Leader Cable", R.A.W. Technical Report # 66065, February 1966.

[6] Madden, P., "CV-880 Rollout Model and Control System", FAA-R.D-72-86, July 1972, pp. 111-127.

[7] Bundick, W.T., "MLS Characteristics", NASA Memorandum, Langley Research Center, September 2, 1975.